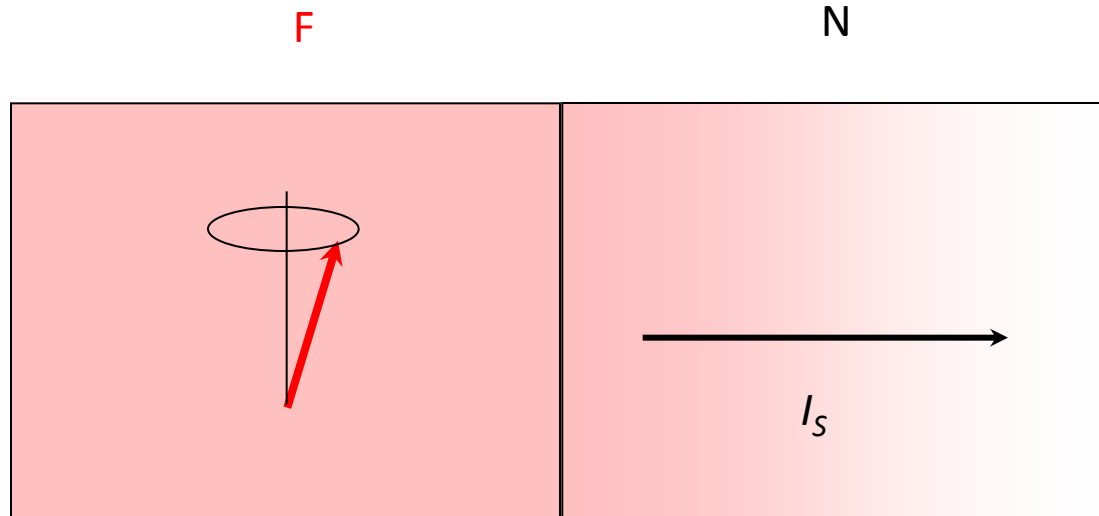


# Spin Pumping



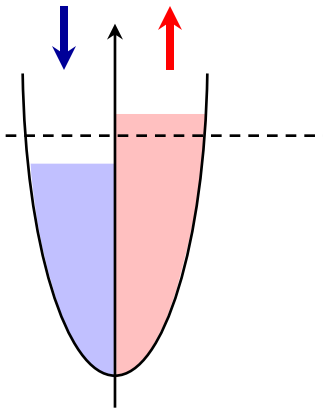
- Landau-Lifshitz-Gilbert

$$\dot{\mathbf{m}} = -\gamma \mathbf{m} \times \mathbf{H}_{\text{eff}} + \mathbf{m} \times (\tilde{\alpha} \dot{\mathbf{m}})$$

$$I_S^{\text{pump}} = \frac{\hbar}{4\pi} g_r^{\downarrow\uparrow} \mathbf{m} \times \frac{\partial \mathbf{m}}{\partial t}$$

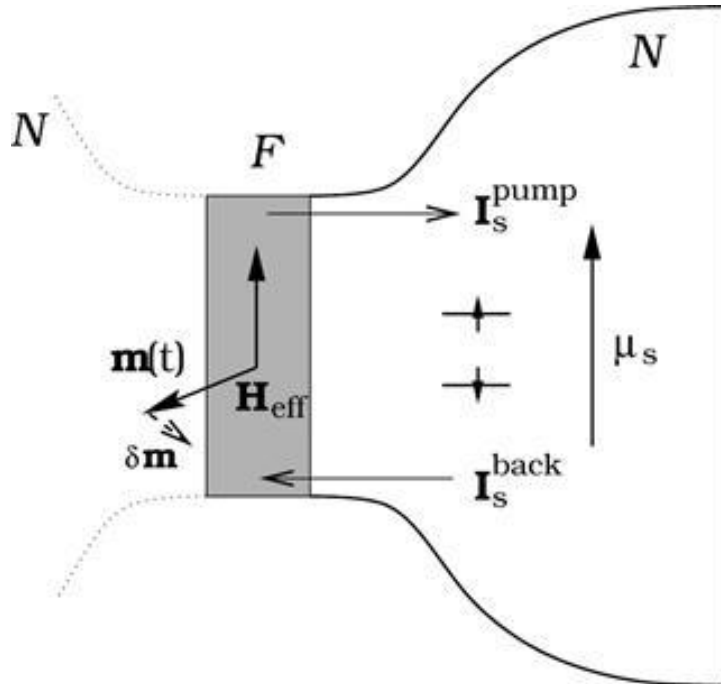
$g_r^{\downarrow\uparrow}$  : spin mixing conductance

Spin accumulation gives rise to **spin current** in neighboring normal metal



In the **FMR condition**, the **steady magnetization precession** in a F is maintained by balancing the absorption of the applied microwave and the **dissipation of the spin angular momentum** --the **transfer of angular momentum** from the local spins to conduction electrons, which **polarizes the conduction-electron spins**.

# Spin Pumping



A ferromagnetic film  $F$  sandwiched between two nonmagnetic reservoirs  $N$ . For simplicity of the discussion in this section, we mainly focus on the dynamics in one (right) reservoir while suppressing the other (left), e.g., assuming it is insulating. The spin-pumping current  $\mathbf{I}_s$  and the spin accumulation  $\mu_s$  in the right reservoir can be found by conservation of energy, angular momentum, and by applying circuit theory to the steady state  $\mathbf{I}_s^{\text{pump}} = \mathbf{I}_s^{\text{back}}$ .

$$\mathbf{I}_s^{\text{pump}} = \frac{\hbar}{4\pi} \left( A_r \mathbf{m} \times \frac{d\mathbf{m}}{dt} - A_i \frac{d\mathbf{m}}{dt} \right).$$

Tserkovnyak *et al*, PRL **88**, 117601 (2002), Enhanced Gilbert Damping in Thin Ferromagnetic Films

Brataas *et al*, PRB **66**, 060404(R) (2002), Spin battery operated by ferromagnetic resonance

Tserkovnyak *et al*, PRB **66**, 224403 (2002), Spin pumping and magnetization dynamics in metallic multilayers

Rev Mod Phys **77**, 1375 (2005) Nonlocal magnetization dynamics in ferromagnetic heterostructures

PRL 110, 217602 (2013)

# Spin Backflow and ac Voltage Generation by Spin Pumping and the Inverse Spin Hall Effect

HuJun Jiao<sup>1</sup> and Gerrit E.W. Bauer<sup>2,1</sup>

<sup>1</sup>Kavli Institute of NanoScience, Delft University of Technology, 2628 CJ Delft, The Netherlands

<sup>2</sup>Institute for Materials Research and WPI-AIMR, Tohoku University, Sendai 980-8577, Japan

(Received 28 September 2012; published 23 May 2013)

The spin current pumped by a precessing ferromagnet into an adjacent normal metal has a constant polarization component parallel to the precession axis and a rotating one normal to the magnetization. The former is now routinely detected as a dc voltage induced by the inverse spin Hall effect (ISHE). Here we compute ac ISHE voltages much larger than the dc signals for various material combinations and discuss optimal conditions to observe the effect. The backflow of spin is shown to be essential to distill parameters from measured ISHE voltages for both dc and ac configurations.

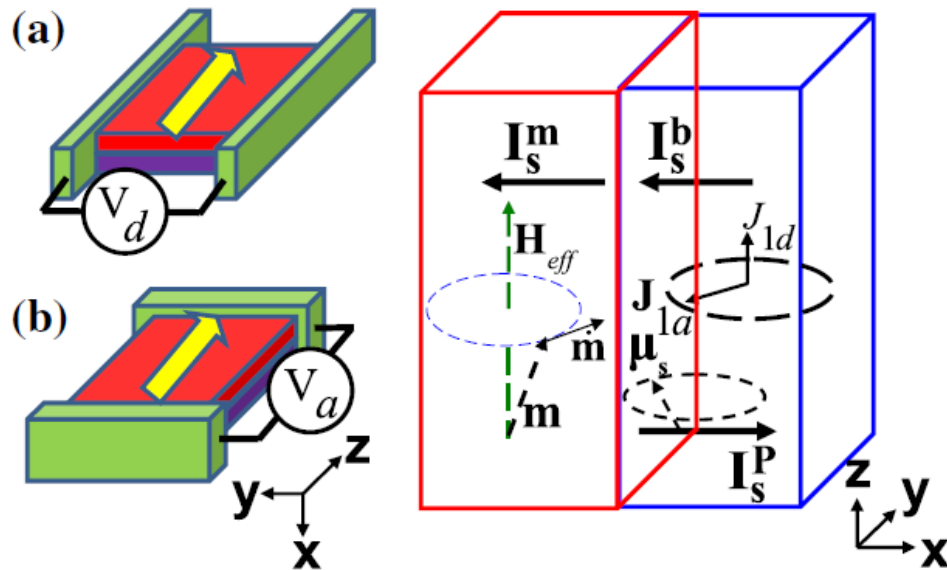
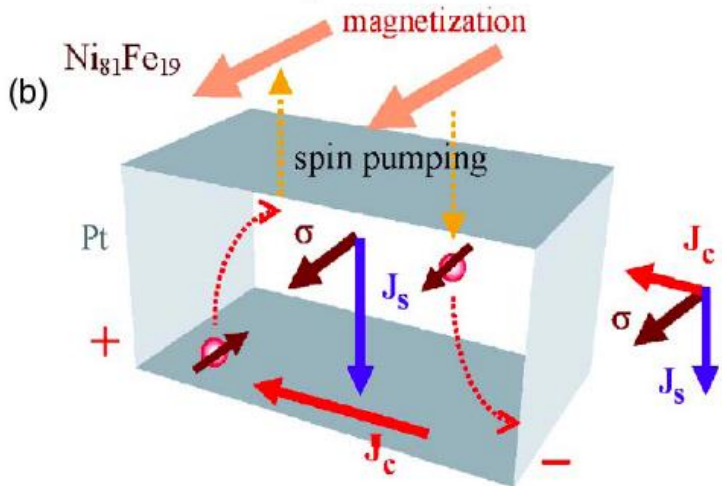
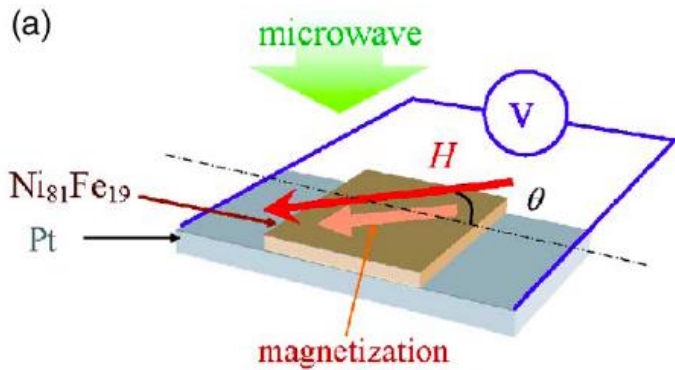


FIG. 1 (color online). Schematic spin battery operated by FMR, for the measurement configurations (a) and (b). The ac (dc) voltage drops along the  $z$  ( $y$ ) direction. The right panel introduces the parameters of the model. The effective field  $\mathbf{H}_{eff}$  is the sum of the external field  $\mathbf{H}_{ex}$  and the uniaxial field  $\mathbf{H}_{un}$ ,  $\mathbf{H}_{ex}$ , and  $\mathbf{H}_{un}$  point along the  $z$  axis. The dc component  $J_{1d}(j_{1s}^z)\mathbf{e}_z$  and ac component  $\mathbf{J}_{1a}(\mathbf{j}_{1s}^a)$  constitute the spin current  $\mathbf{j}_{1s}$ .

# Combining Spin Pumping and Inverse Spin Hall Effect



FMR



Spin Current

in adjacent  
normal metal



Transverse  
Charge Current

The spin-orbit interaction bends these two electrons in the same direction and induces a charge current transverse to  $J_s$ ,

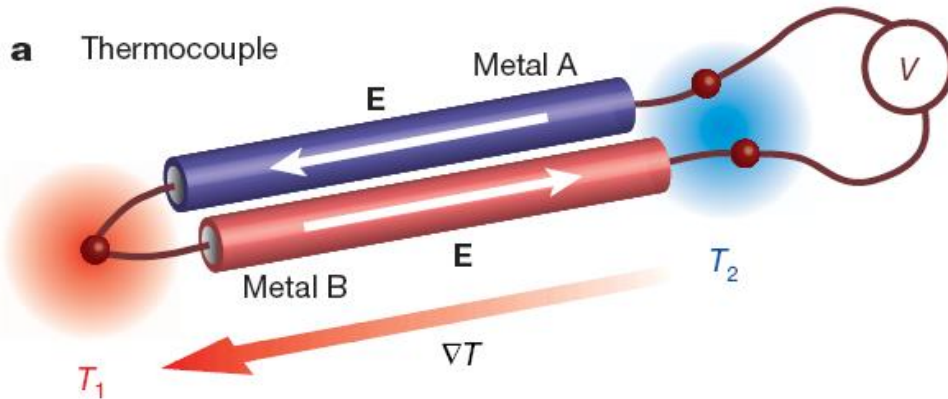
$$J_c = D_{ISHE} J_s \times \sigma.$$

The surface of the Pt layer is of a  $1 \times 1 \text{ mm}^2$  square shape. Two electrodes are attached to both ends of the Pt layer.

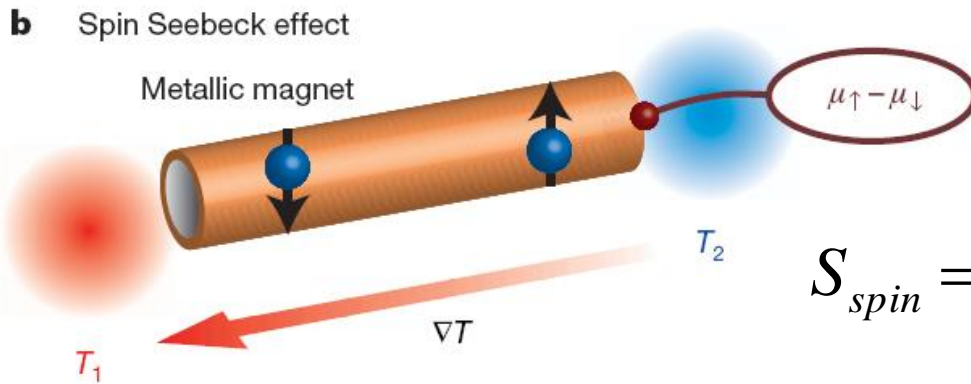
Saitoh *et al*, APL **88**, 182509 (2006)

Kimura *et al*, PRL **98**, 156601 (2007)

# Spin Seebeck effect



$$\delta V = S \delta T$$



$$\delta V_{spin} = S_{spin} \delta T$$

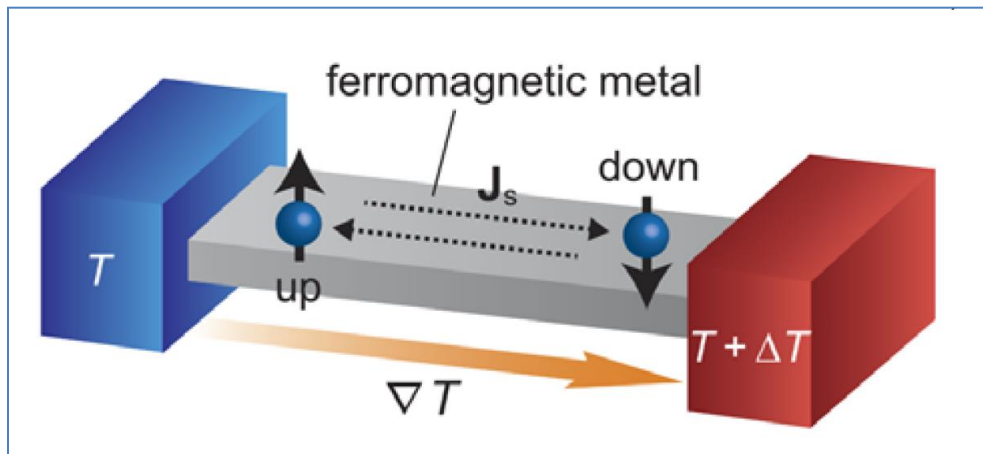
$$S_{spin} = (1/e) [\partial \mu_{\uparrow}^c / \partial T - \partial \mu_{\downarrow}^c / \partial T]$$

# Spin Seebeck effect

In a ferromagnetic metal, **up-spin** and **down-spin conduction** electrons have **different scattering rates and densities**, and thus have different Seebeck coefficients.

$$\mathbf{j}_s = \mathbf{j}_\uparrow - \mathbf{j}_\downarrow = (\sigma_\uparrow \mathbf{S}_\uparrow - \sigma_\downarrow \mathbf{S}_\downarrow)(-\nabla T)$$

This **spin current** flows **without accompanying charge currents** in the open-circuit condition, and the up-spin and down-spin currents flow **in opposite directions** along the temperature gradient

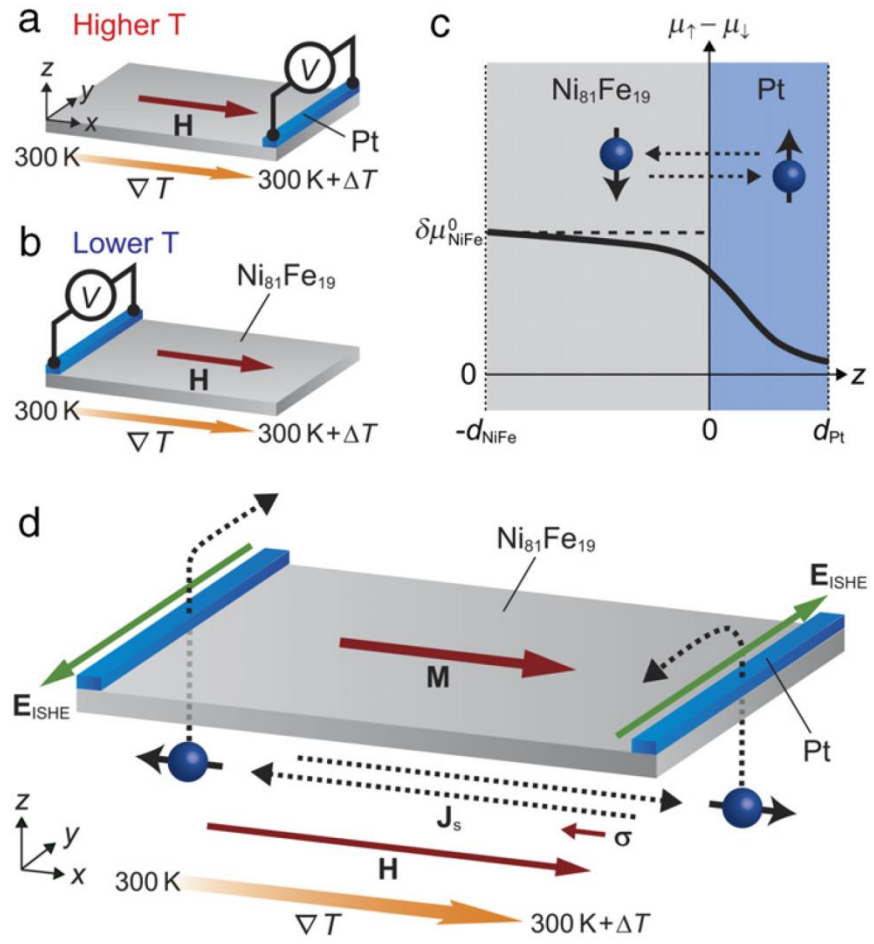
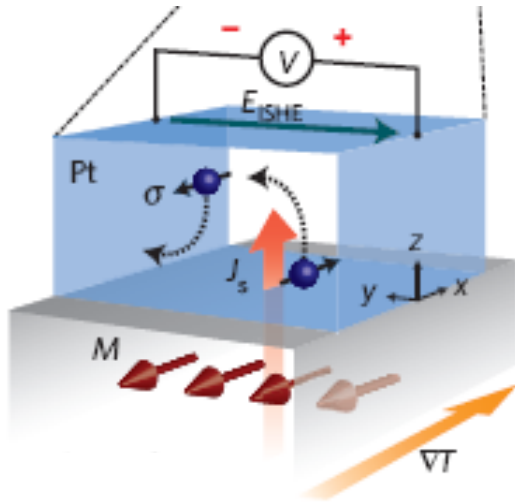


How to detect  $j_s$  ?

Inverse Spin Hall Effect converts  $j_s$  into  $j_c$

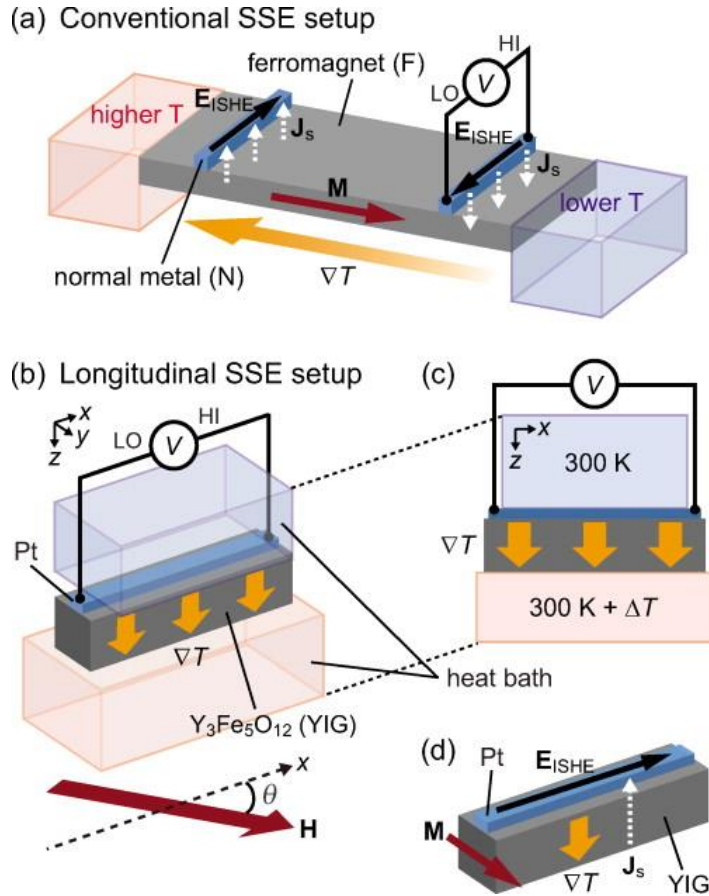
# Detection of Spin Current by Inverse Spin Hall Effect

The ISHE converts a spin current into an **electromotive force**  $E_{SHE}$  by means of **spin-orbit scattering**.

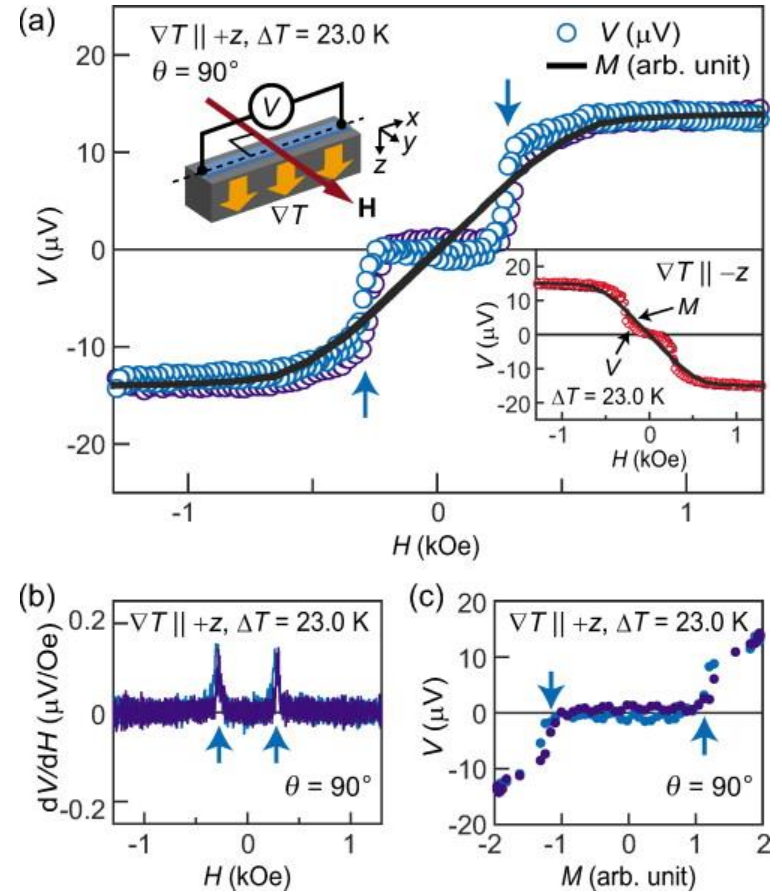


$$E_y = E_{SHE} = D_{ISHE} J_S \times \sigma$$

A spin current carries a **spin-polarization vector**  $\sigma$  along a spatial direction  $J_S$ .



(a) A schematic of the conventional setup for measuring the ISHE induced by the SSE. Here,  $\nabla T$ ,  $M$ ,  $J_s$ , and  $E_{ISHE}$  denote a temperature gradient, the magnetization vector of a ferromagnet (F), the spatial direction of the spin current flowing across the F/no...



(a) Comparison between the  $H$  dependence of  $V$  at  $\Delta T = 23.0$  K in the YIG/Pt system and the magnetization  $M$  curve of the YIG. During the  $V$  measurements,  $\nabla T$  was applied along the  $+z$  direction [the  $-z$  direction for the inset to (a)] and  $H$  was applied along the...

Uchida et al, APL 97, 172505 (2010)

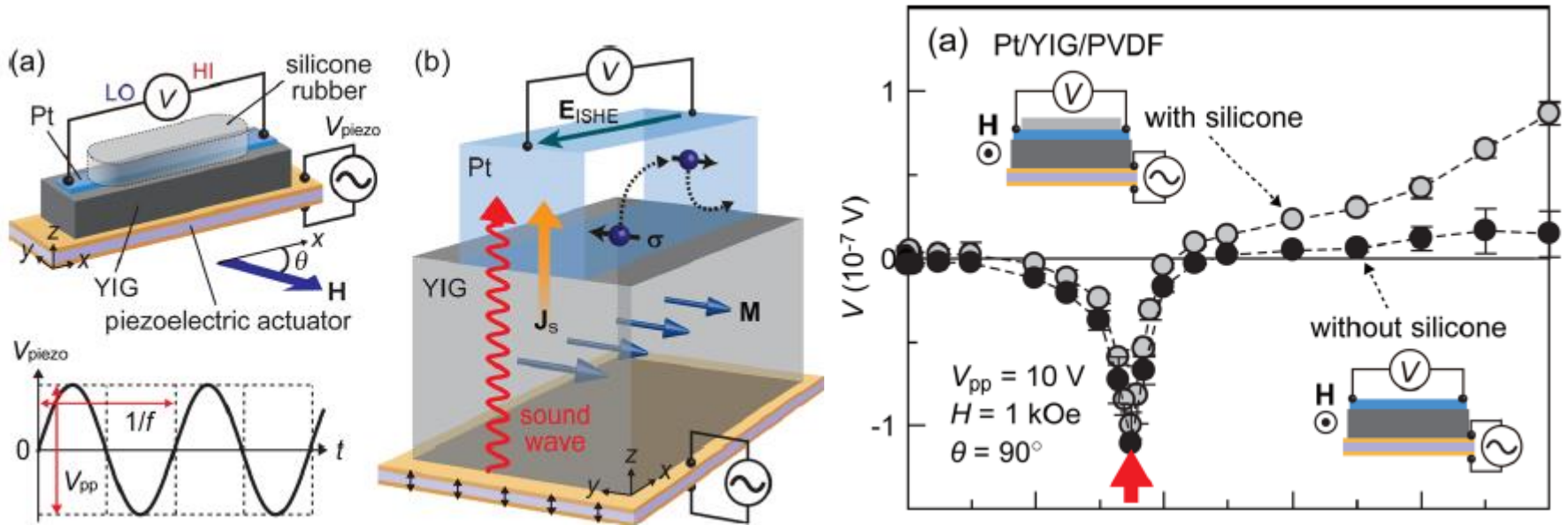
© 2010 American Institute of Physics

# sound waves

JOURNAL OF APPLIED PHYSICS **111**, 053903 (2012)

## Acoustic spin pumping: Direct generation of spin currents from sound waves in Pt/Y<sub>3</sub>Fe<sub>5</sub>O<sub>12</sub> hybrid structures

K. Uchida,<sup>1,2,a)</sup> H. Adachi,<sup>2,3</sup> T. An,<sup>1,2</sup> H. Nakayama,<sup>1,2</sup> M. Toda,<sup>4</sup> B. Hillebrands,<sup>5</sup>  
S. Maekawa,<sup>2,3</sup> and E. Saitoh<sup>1,2,3</sup>

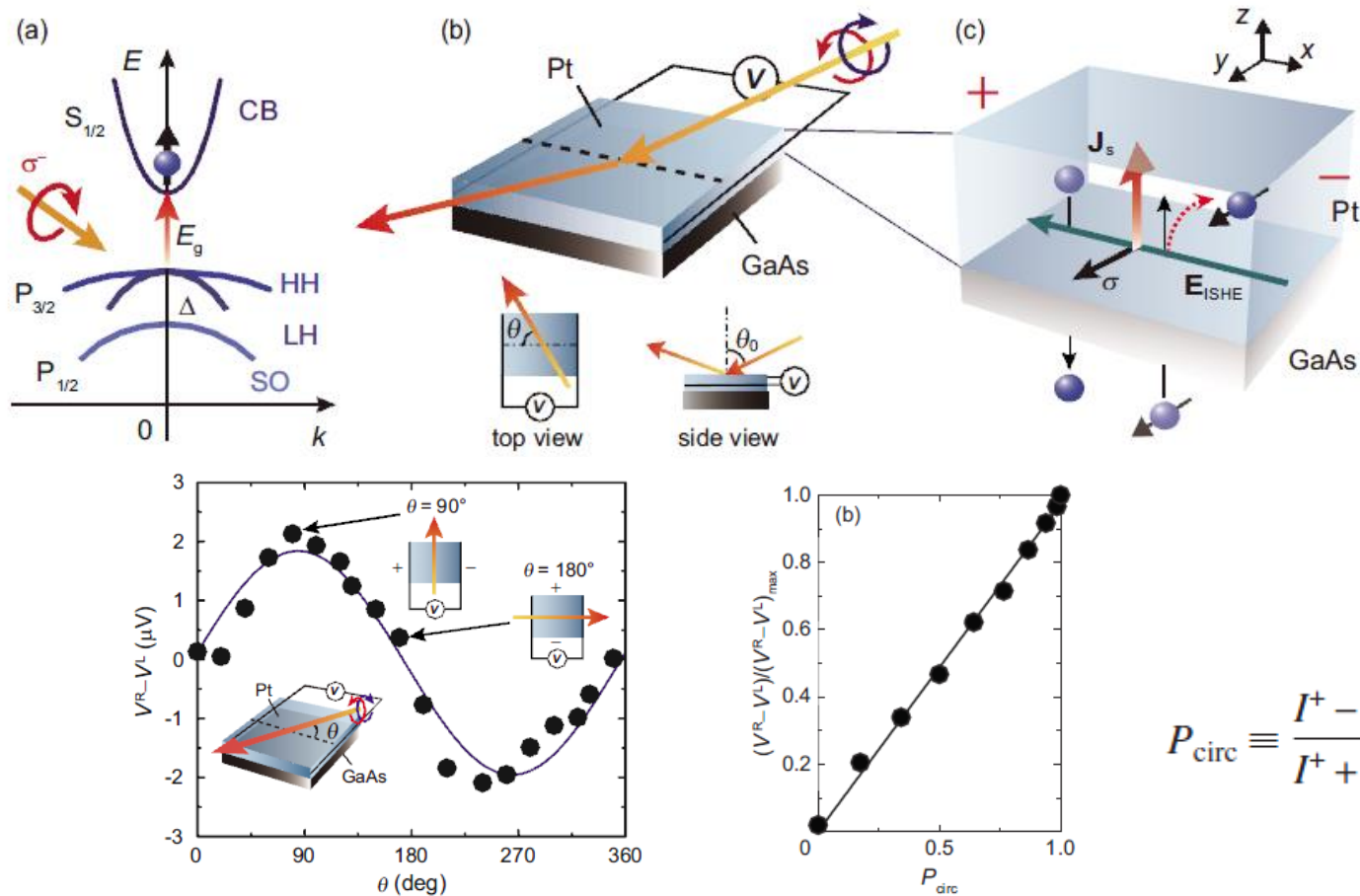


# circularly polarized light

APPLIED PHYSICS LETTERS 96, 082502 (2010)

## Photoinduced inverse spin-Hall effect: Conversion of light-polarization information into electric voltage

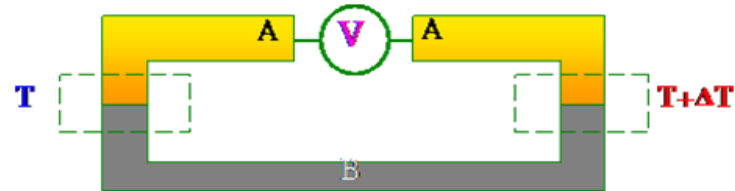
K. Ando,<sup>1,2,a)</sup> M. Morikawa,<sup>2</sup> T. Trypiniotis,<sup>3</sup> Y. Fujikawa,<sup>1</sup> C. H. W. Barnes,<sup>3</sup> and E. Saitoh<sup>1,2,4</sup>



# Thermoelectric effect:

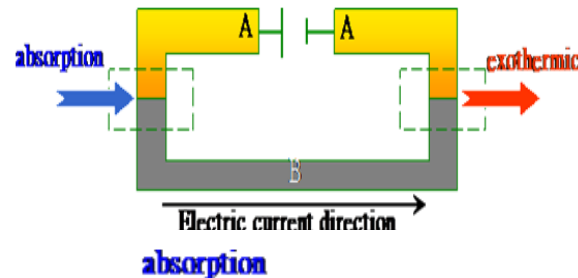
The thermoelectric effect is the direct conversion of temperature differences to electric voltage and vice-versa.

→ Seebeck effect (1821):



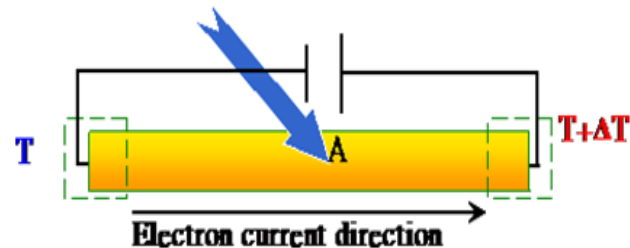
$$\Delta T \rightarrow V$$

→ Peltier effect (1823):



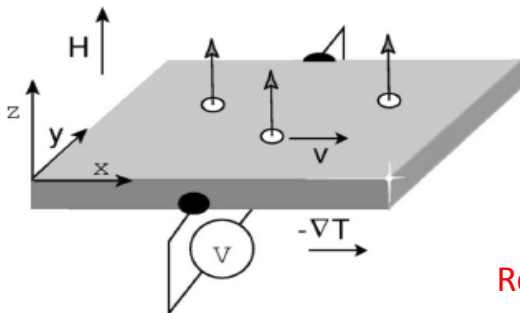
$$I \rightarrow Q$$

→ Thomson effect (1851):



$$I + \Delta T \rightarrow Q$$

Nernst effect :

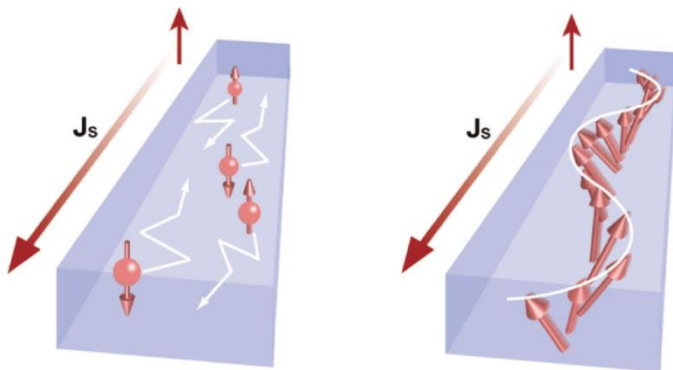
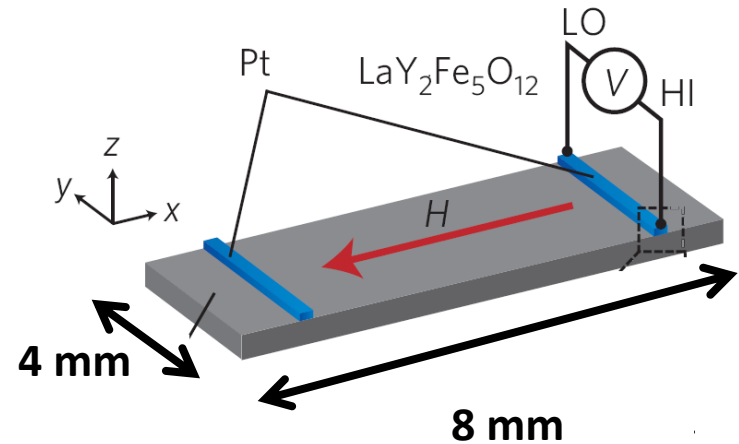
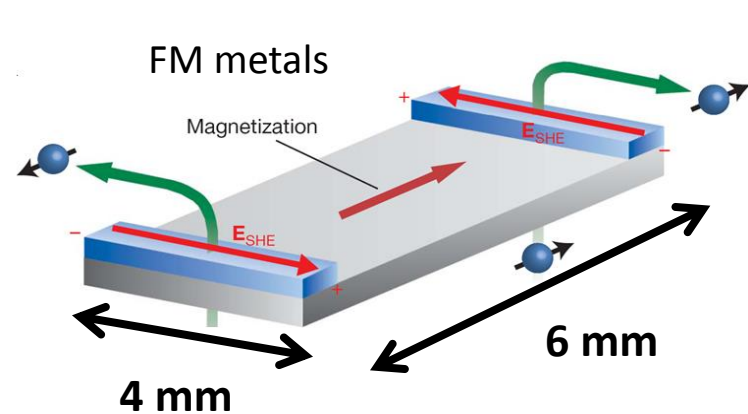


When a sample is subjected to a magnetic field and a temperature gradient normal (perpendicular) to each other, an electric field will be induced normal to both.

# Mystery 1:

## Transmission of Spin Current in Metal and Insulator

Over macroscopic distance ( $\text{mm's} \gg \text{spin diffusion length}$ ) without dissipation ?

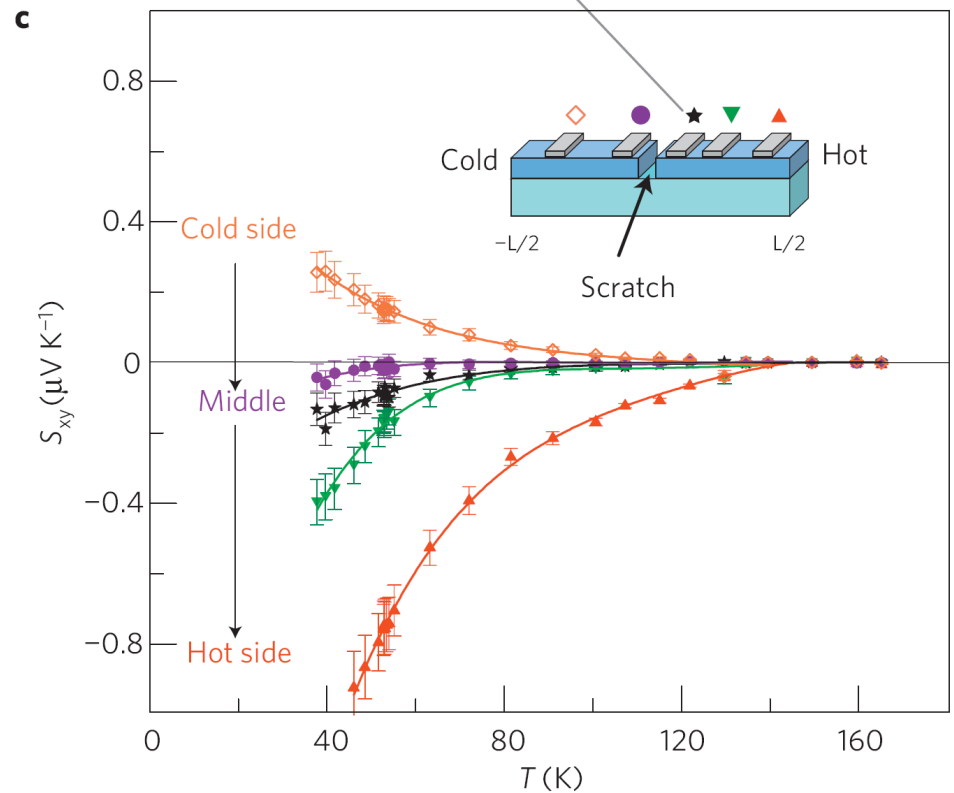
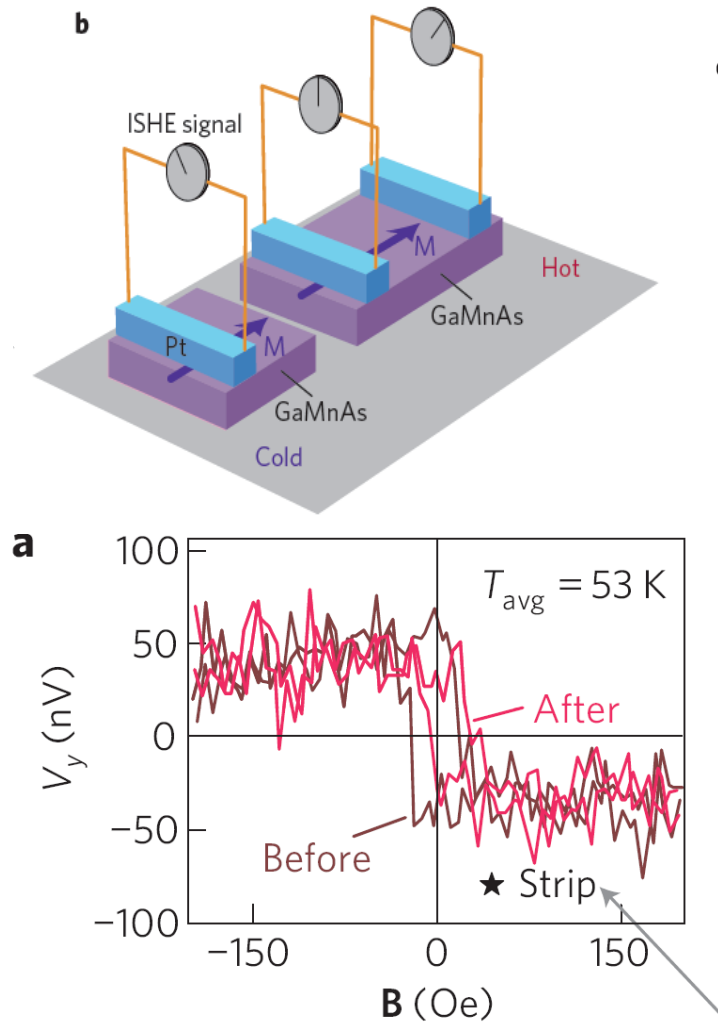


Conduction-electron  
spin current

Spin-wave  
spin current

Resolution: Transmission of spin currents by **magnons (spin waves)** in either FM metals or FM insulators

# Mystery 2: Spin Seebeck effect in **broken** FM semiconductor

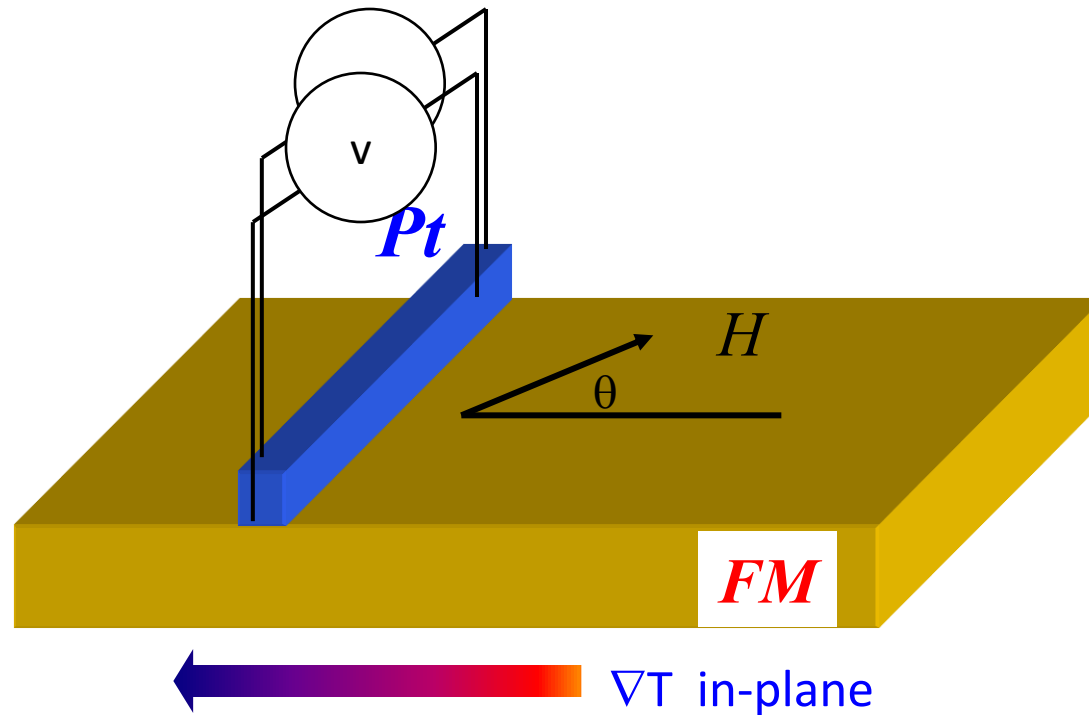


Transmission of spin currents ?

**Intrinsic Caloritronic effects (not substrate dominated) ?**

**Intrinsic spin Seebeck effect ?**

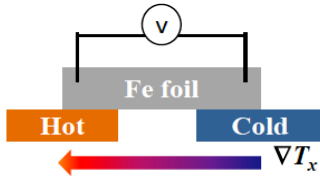
**Intrinsic spin-dependent thermal transport ?**



Huang, Wang, Lee, Kwo, and CLC,

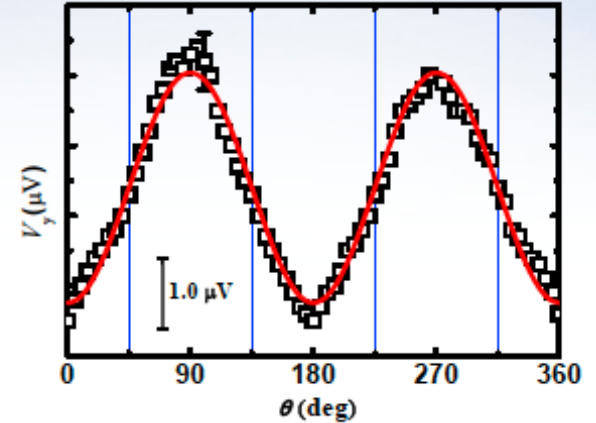
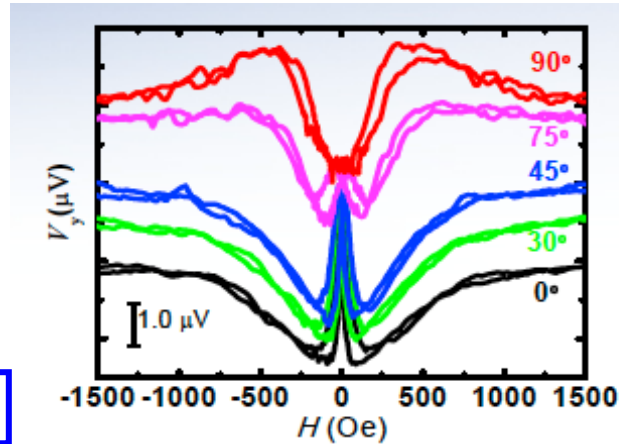
“Intrinsic spin-dependent thermal transport,” PRL **107**, 216604 (2011).

# Intrinsic spin caloritronic properties with in-plane $\nabla_x T$

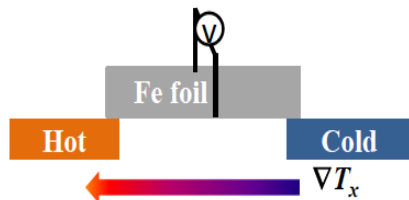


Longitudinal voltage:  
thermal AMR

$$V_{th} = V_{th\perp} + (V_{th\perp} - V_{th\parallel})\cos^2\theta_M$$

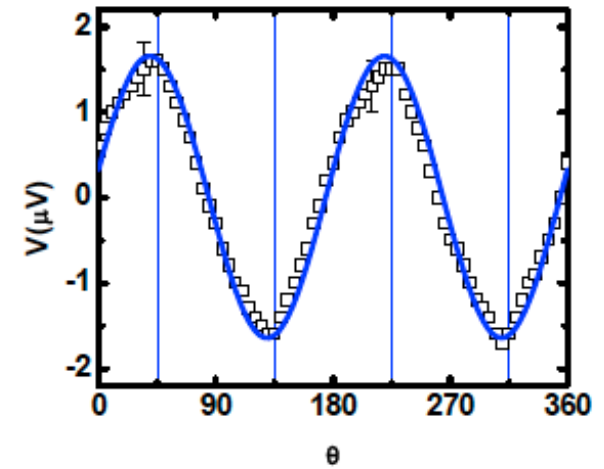
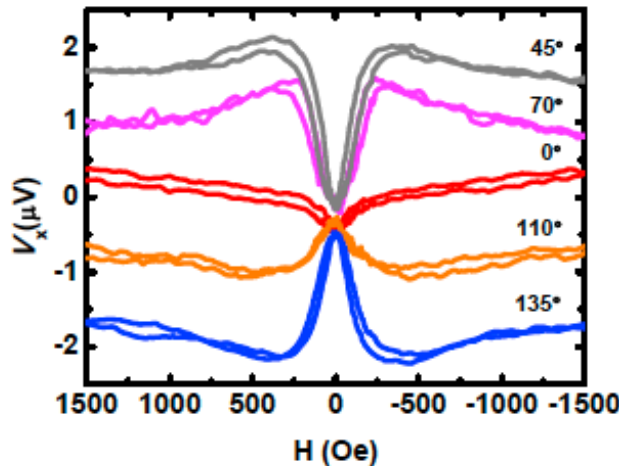


Symmetric in H !



Transverse voltage:  
Planar Nernst effect

$$\sin 2\theta_M$$



**Necessary Signatures of FM film with in-plane  $\nabla_x T$**

1. Thin film/substrate, in-plane ( $\nabla_x T$ ) **and** perpendicular ( $\nabla_z T$ )

Spin Seebeck effect  
( $\nabla_x T$ ) with Pt

Anomalous Nernst effect  
( $\nabla_z T$ ) with or without Pt

2.  $V_{ANE}$  and  $(V_{SSE})_{Pt}$  are **additive**

If  $V_{ANE}$  unknown,  $(V_{SSE})_{Pt}$  uncertain

**Intrinsic spin Seebeck effect ?**

3. ANE: excellent detector of  $\nabla_z T$  and  $\Delta T_z$

4. Intrinsic spin caloritronics with in-plane  $\nabla_x T$  in Fe foils

Thermal AMR ( $\cos^2 \theta$ )

Planar Nernst ( $\sin 2\theta$ )

**Necessary conditions for in-plane  $\nabla_x T$  only**

# Topological insulator

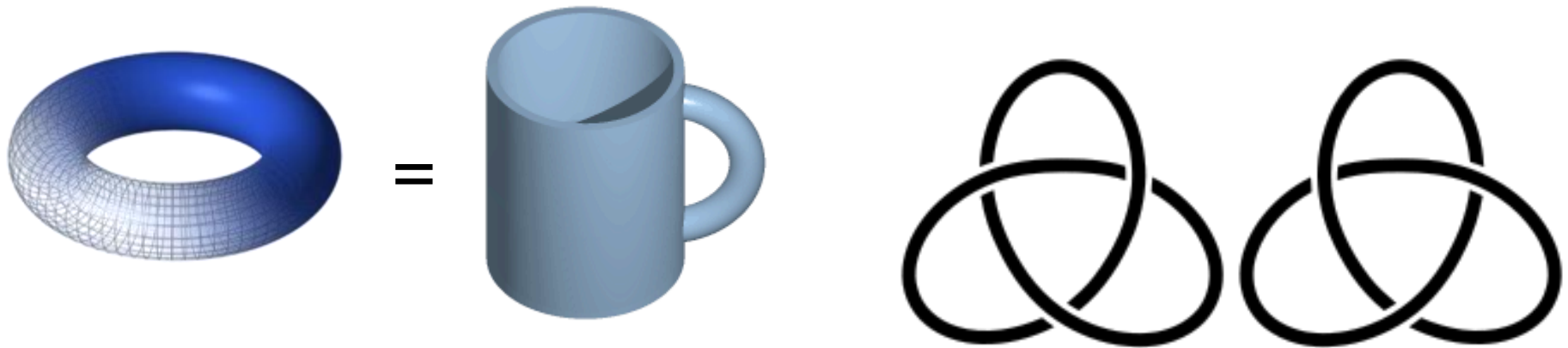


- A topological insulator is a material **conducting** on its boundary but behaves as an **insulator** in its bulk.
- The conducting channel(s) are guaranteed by **time-reversal symmetry**, topologically protected, will not be affected by local impurities etc, and thus robust.

# Why the word 'topological'?

- Topological order: a pattern of long-range quantum entanglement in quantum states, can be described by a new set of quantum numbers, such as ground state degeneracy, quasiparticle fractional statistics, edge states, topological entropy, etc.

- Landau symmetry breaking  
describes classical orders in materials. But it failed to describe the chiral spin state, which was proposed (but failed) to explain HTS.



- $Z_2$  topological quantum number
- Chern numbers (陳省身) explains Quantum Hall Effect [\(from Foucault pendulum to Chern numbers\)](#)

$$\frac{1}{2\pi} \int_S K dA = 2(1 - g)$$

How to become a topological insulator?

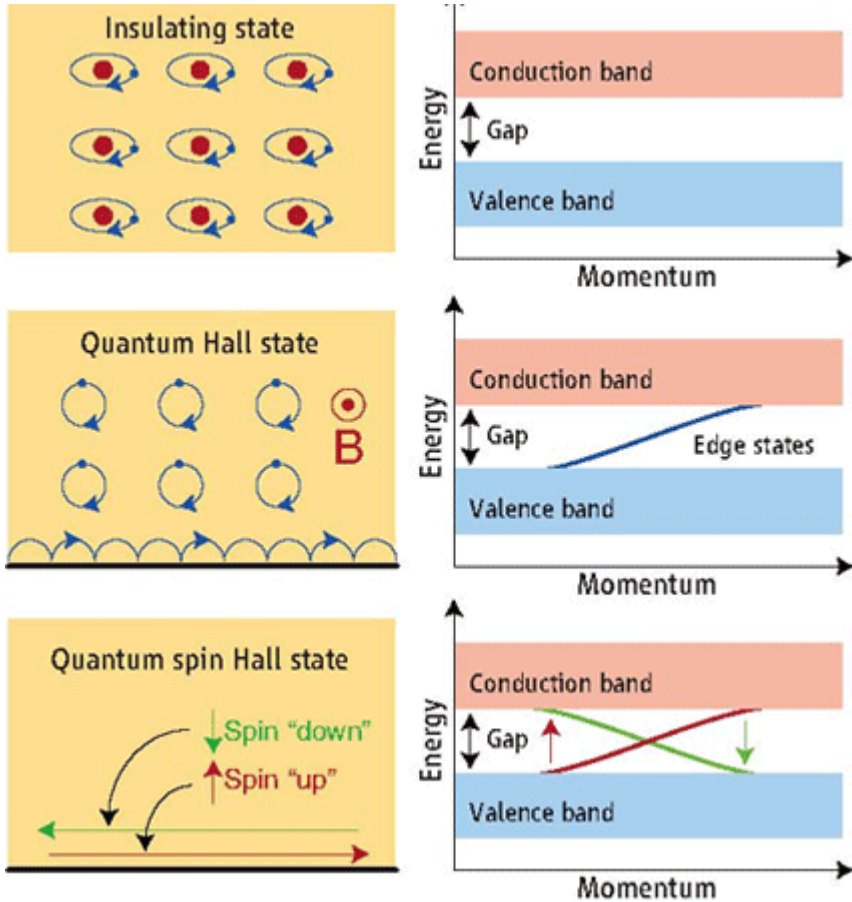
Or, how to cross from an intrinsic insulator to a topological insulator?

Or, how to build the edge conducting states?

- Spin-orbit effect
- Lattice constant adjustment

To get inversion states and Dirac cone on the boundary.

- Carriers in these states have their spin locked at a **right-angle** to their **momentum**. At a given energy the only other available electronic states have opposite spin, so scattering is strongly suppressed and conduction on the surface is nearly **dissipationless**.



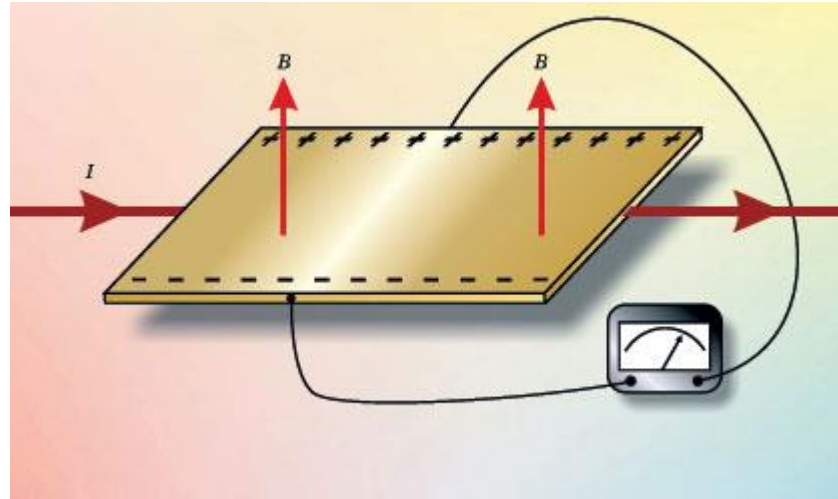
- States of matter. **(Top)** Electrons in an insulator are bound in localized orbitals (left) and have an energy gap (right) separating the occupied valence band from the empty conduction band. **(Middle)** A two-dimensional quantum Hall state in a strong magnetic field has a bulk energy gap like an insulator but permits electrical conduction in one-dimensional “one way” edge states along the sample boundary. **(Bottom)** The quantum spin Hall state at zero magnetic field also has a bulk energy gap but allows conduction in spin-filtered edge states.

# A zoo of Hall effects

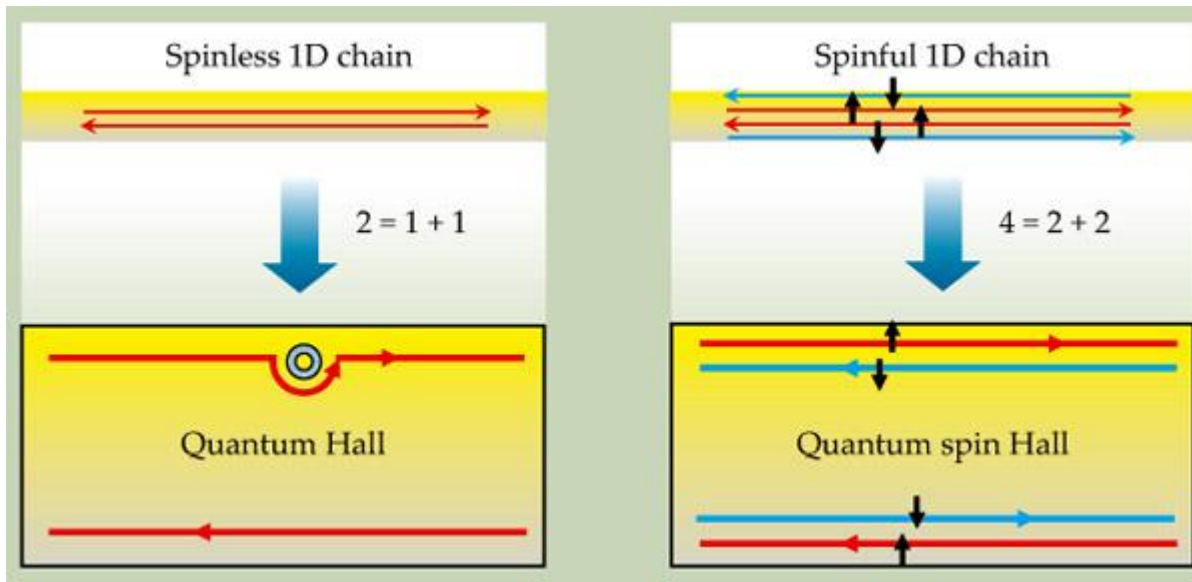
- Hall effect ---  $B \perp I, V \perp I$
- Anomalous (Extra-ordinary) Hall effect ---  
extra voltage proportional to magnetization
- Planar Hall effect --- in-plane field,  $V \perp I$
- (Integer) Quantum Hall effect ---  
 $B \perp I, V \perp I$  in 2D electron gas
- Fractional Quantum Hall effect ---  
electrons bind magnetic flux lines
- Spin Hall effect ---  $B = 0, V \perp I$
- Quantum Spin Hall effect --- 2D topological insulator

$$R_H = \frac{-n\mu_e^2 + p\mu_h^2}{e(n\mu_e + p\mu_h)^2}$$

$$\sigma = \nu \frac{e^2}{h},$$



Edwin Hall's 1878 experiment was the first demonstration of the Hall effect. A magnetic field  $B$  normal to a gold leaf exerts a Lorentz force on a current  $I$  flowing longitudinally along the leaf. That force separates charges and builds up a transverse "Hall voltage" between the conductor's lateral edges. Hall detected this transverse voltage with a voltmeter that spanned the conductor's two edges.



PhysicsToday, Jan 2010, p33

**Figure 1. Spatial separation** is at the heart of both the quantum Hall (QH) and the quantum spin Hall (QSH) effects. **(a)** A spinless one-dimensional system has both a forward and a backward mover. Those two basic degrees of freedom are spatially separated in a QH bar, as illustrated by the symbolic equation “ $2 = 1 + 1$ .” The upper edge contains only a forward mover and the lower edge has only a backward mover. The states are robust: They will go around an impurity without scattering. **(b)** A spinful 1D system has four basic channels, which are spatially separated in a QSH bar: The upper edge contains a forward mover with up spin and a backward mover with down spin, and conversely for the lower edge. That separation is illustrated by the symbolic equation “ $4 = 2 + 2$ .”

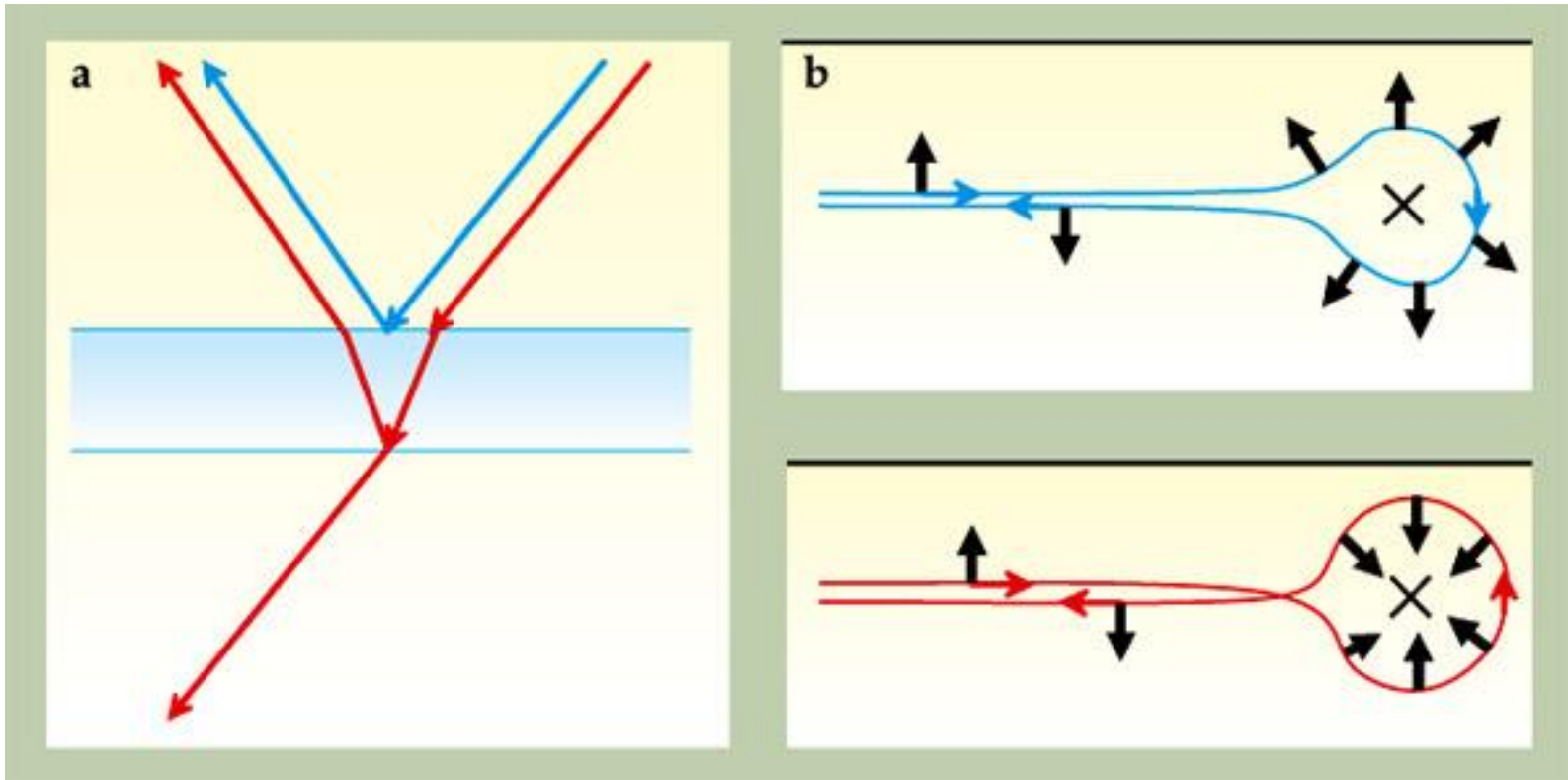


**Figure 2. (a)** On a lens with antireflection coating, light waves reflected by the top (blue line) and the bottom (red line) surfaces interfere destructively, which leads to suppressed reflection. **(b)** A quantum spin Hall edge state can be scattered in two directions by a nonmagnetic impurity. Going clockwise along the blue curve, the spin rotates by  $\pi$ ; counterclockwise along the red curve, by  $-\pi$ . A quantum mechanical phase factor of  $-1$  associated with that difference of  $2\pi$  leads to destructive interference of the two paths—the backscattering of electrons is suppressed in a way similar to that of photons off the antireflection coating.

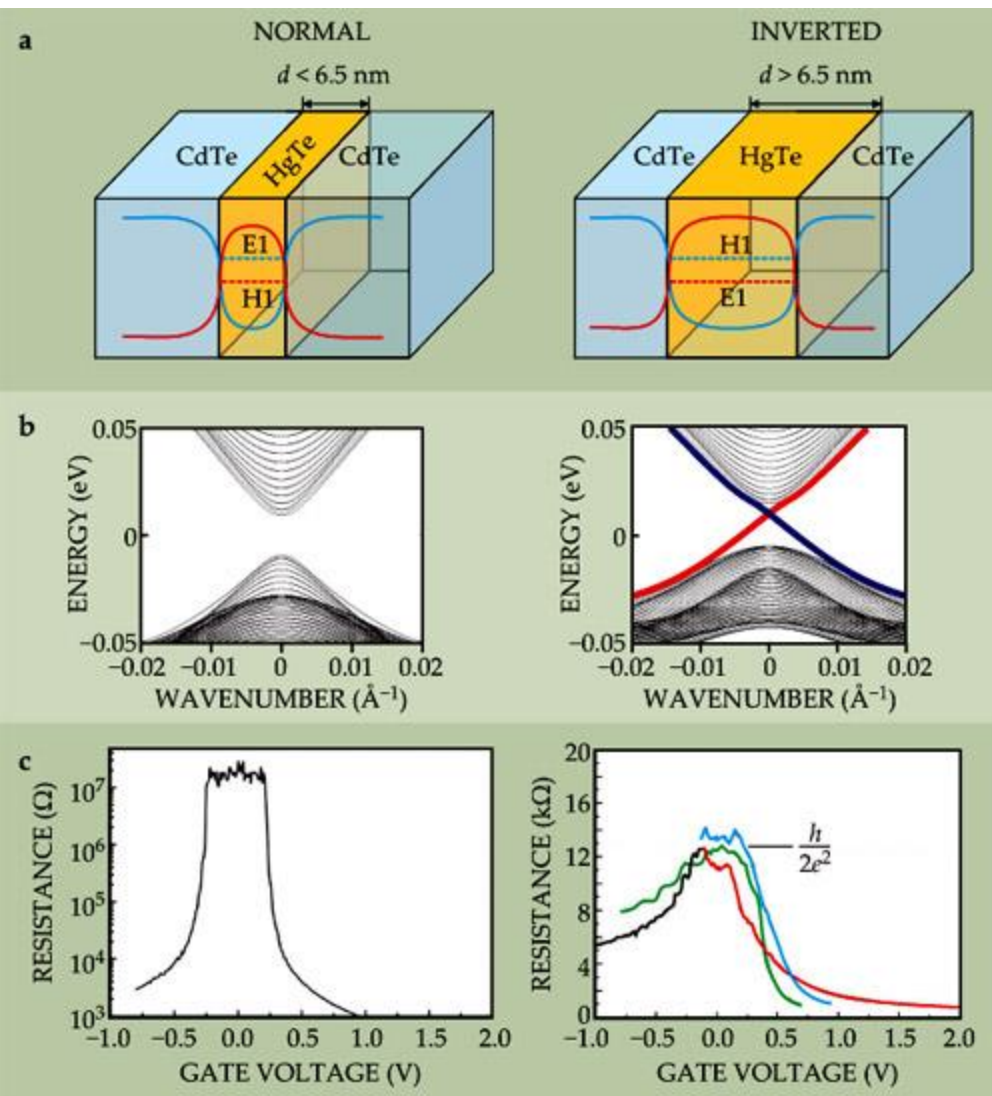
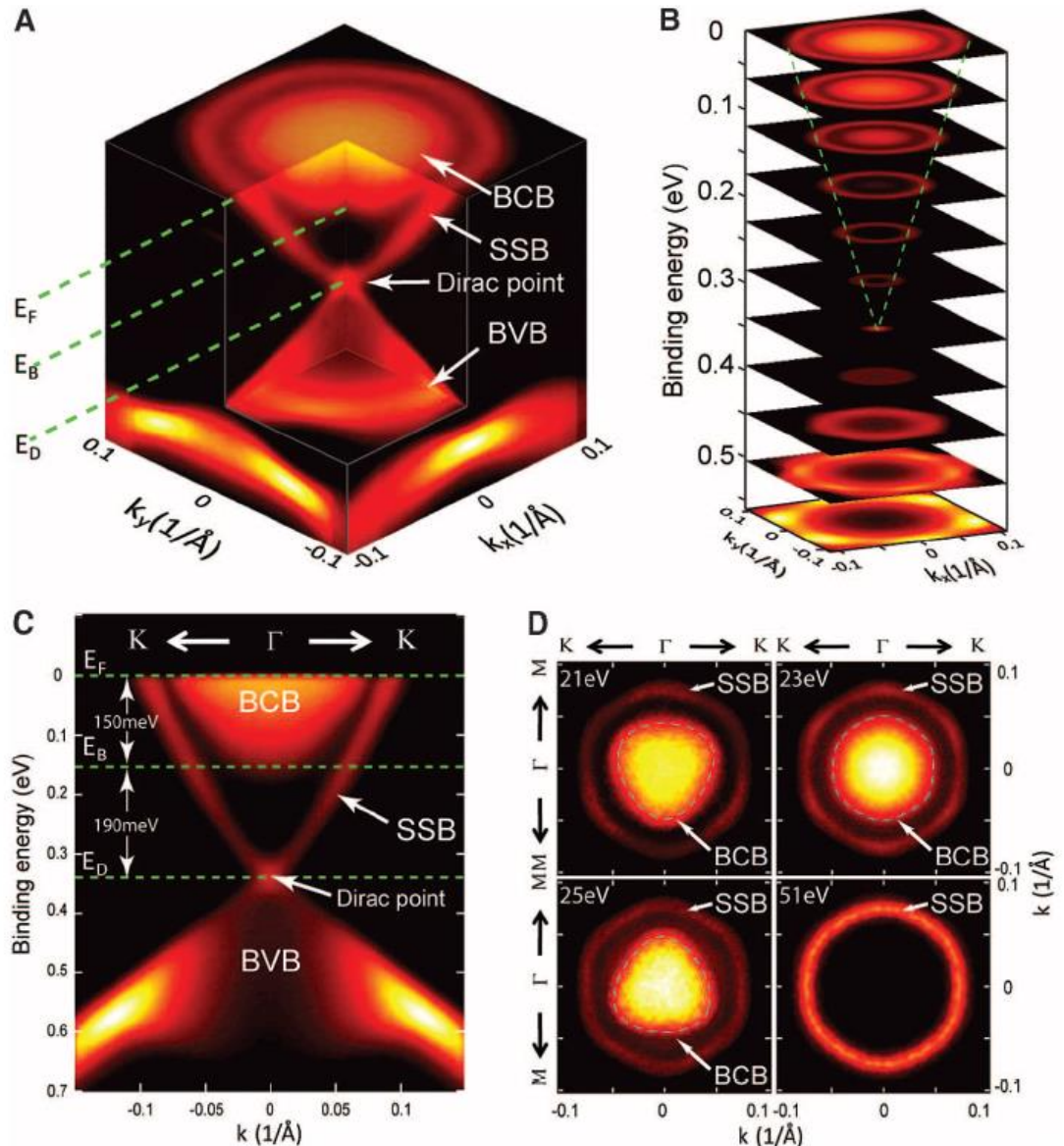


**Figure 3. Mercury telluride quantum wells** are two-dimensional topological insulators. **(a)** The behavior of a mercury telluride–cadmium telluride quantum well depends on the thickness  $d$  of the HgTe layer. Here the blue curve shows the potential-energy well experienced by electrons in the conduction band; the red curve is the barrier for holes in the valence band. Electrons and holes are trapped laterally by those potentials but are free in the other two dimensions. For quantum wells thinner than a critical thickness  $d_c \approx 6.5$  nm, the energy of the lowest-energy conduction subband, labeled E1, is higher than that of the highest-energy valence band, labeled H1. But for  $d > d_c$ , those electron and hole bands are inverted. **(b)** The energy spectra of the quantum wells. The thin quantum well has an insulating energy gap, but inside the gap in the thick quantum well are edge states, shown by red and blue lines. **(c)** Experimentally measured resistance of thin and thick quantum wells, plotted against the voltage applied to a gate electrode to change the chemical potential. The thin quantum well has a nearly infinite resistance within the gap, whereas the thick quantum well has a quantized resistance plateau at  $R = h/2e^2$ , due to the perfectly conducting edge states. Moreover, the resistance plateau is the same for samples with different widths, from 0.5  $\mu\text{m}$  (red) to 1.0  $\mu\text{m}$  (blue), proof that only the edges are conducting.

# Angle Resolved Photo Emission Spectroscopy (ARPES)

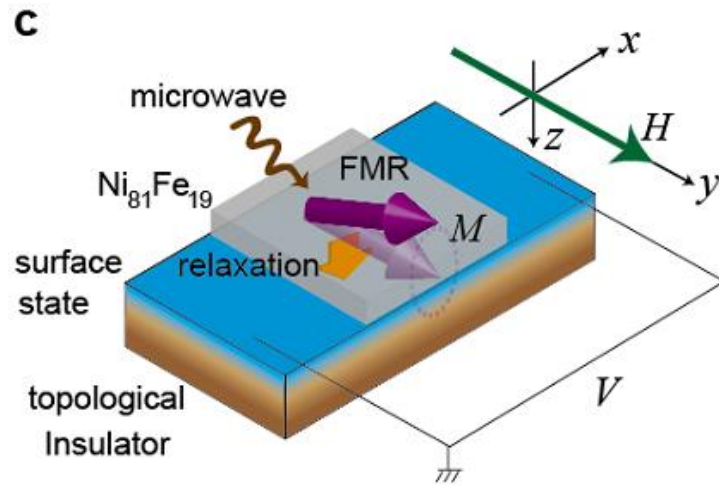
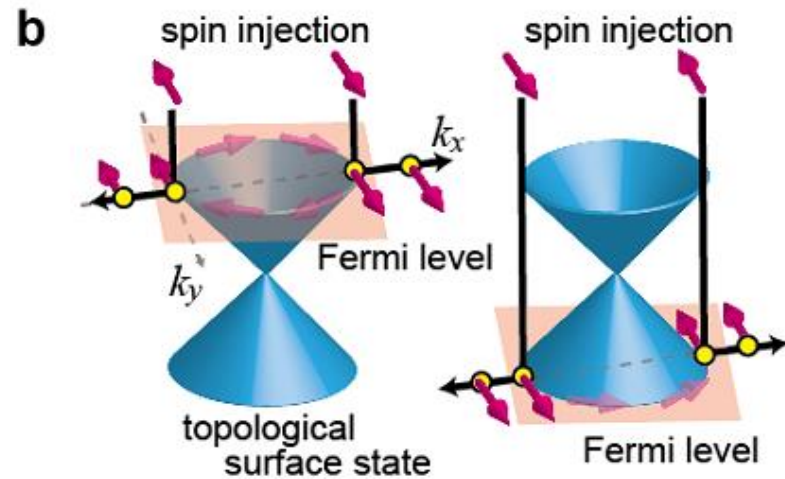
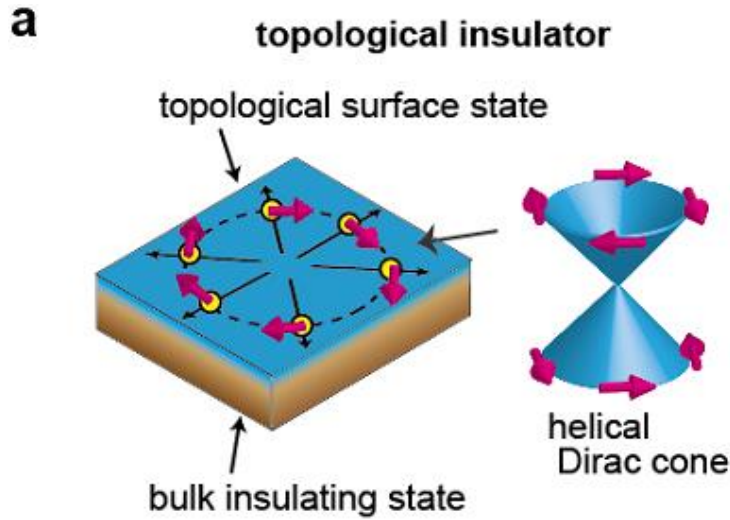
**Fig. 1.** Electronic band structure of undoped  $\text{Bi}_2\text{Se}_3$  measured by ARPES. **(A)** The bulk conduction band (BCB), bulk valence band (BVB), and surface-state band (SSB) are indicated, along with the Fermi energy ( $E_F$ ), the bottom of the BCB ( $E_B$ ), and the Dirac point ( $E_D$ ). **(B)** Constant-energy contours of the band structure show the SSB evolution from the Dirac point to a hexagonal shape (green dashed lines). **(C)** Band structure along the  $\text{K}-\Gamma-\text{K}$  direction, where  $\Gamma$  is the center of the hexagonal surface Brillouin zone (BZ), and the  $\text{K}$  and  $\text{M}$  points [see (D)] are the vertex and the midpoint of the side of the BZ, respectively (14). The BCB bottom is  $\sim 190$  meV above  $E_D$  and 150 meV below  $E_F$ . **(D)** Photon energy-dependent FS maps (symmetrized according to the crystal symmetry). Blue dashed lines around the BCB FS pocket indicate their different shapes.



3 D topological insulators:  
 $\text{Bi}_2\text{Sb}_3$ ,  $\text{Bi}_2\text{Se}_3$ ,  $\text{Bi}_2\text{Te}_3$ ,  
 $\text{Sb}_2\text{Te}_3$ . There is optical  
 proof of the Dirac cone,  
 but no transport evidence.

[M. Z. Hasan](#), [C. L. Kane](#)

# Topological insulators for Spintronic



A. TIs have topologically-protected metallic surface states.

spin-momentum locking: Conduction electron states behave as Dirac fermions.

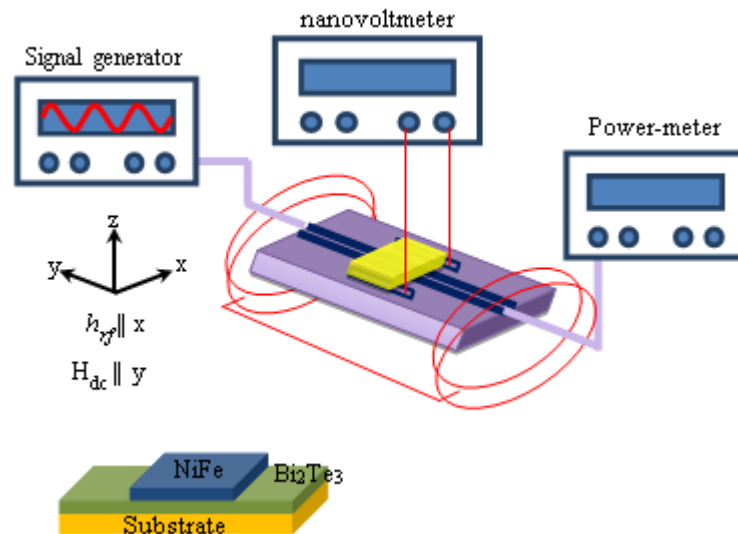
B. i.e. direction of the e-motion determines its spin direction.

C. if a spin imbalance is induced in the surface state by spin pumping, a charge current  $J_c$  is expected to show up along the "Hall" direction defined by  $J_c \parallel (z \times \sigma)$

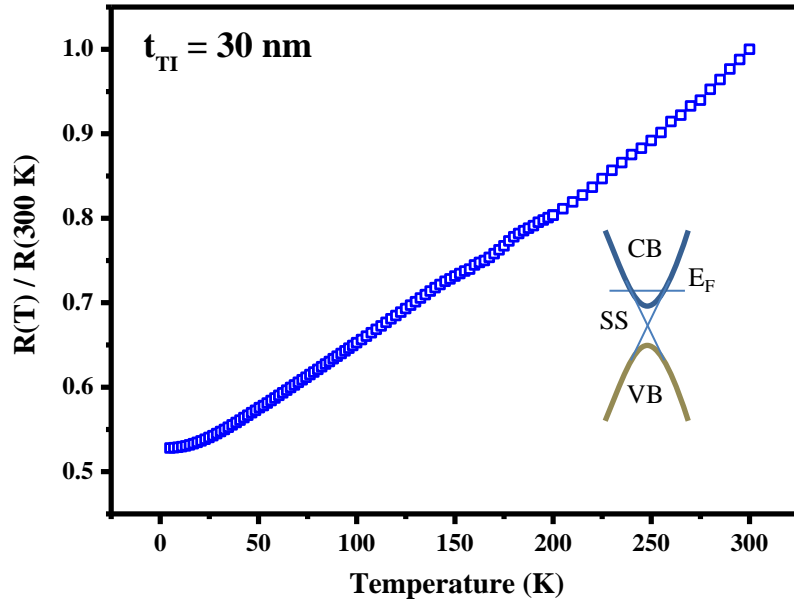
# Spin Chemical Potential Bias Induced Surface Current Evidenced by Spin Pumping into Topological Insulator $\text{Bi}_2\text{Te}_3$

Faris Basheer Abdulahad, Jin-Han Lin, Yung Liou, Wen-Kai Chiu, Liang-Juan Chang, Ming-Yi Kao, Jun-Zhi Liang, Dung-Shing Hung, and Shang-Fan Lee

PRB Rapid Comm. **92**, 241304R (2015)

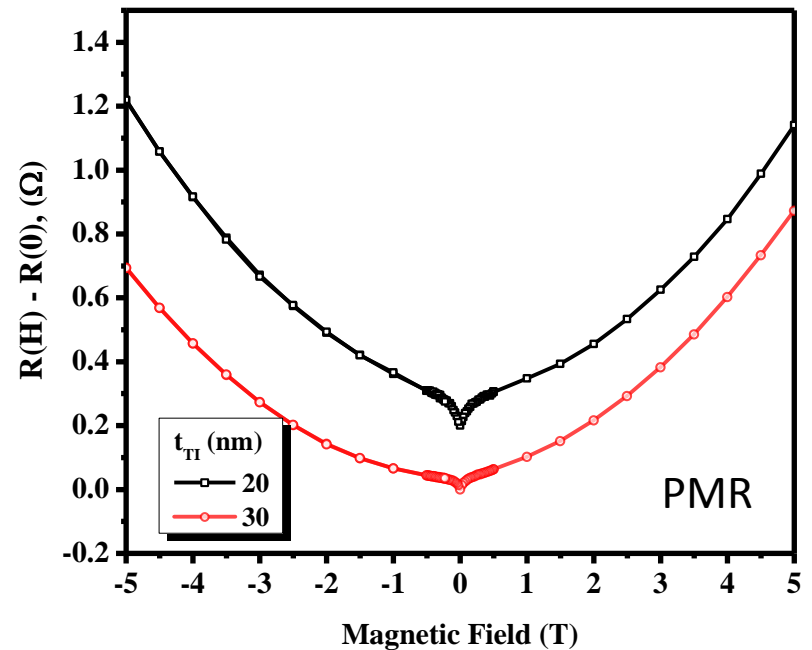


# Transport measurements on $\text{Bi}_2\text{Te}_3$ films grown on sapphire (0001)

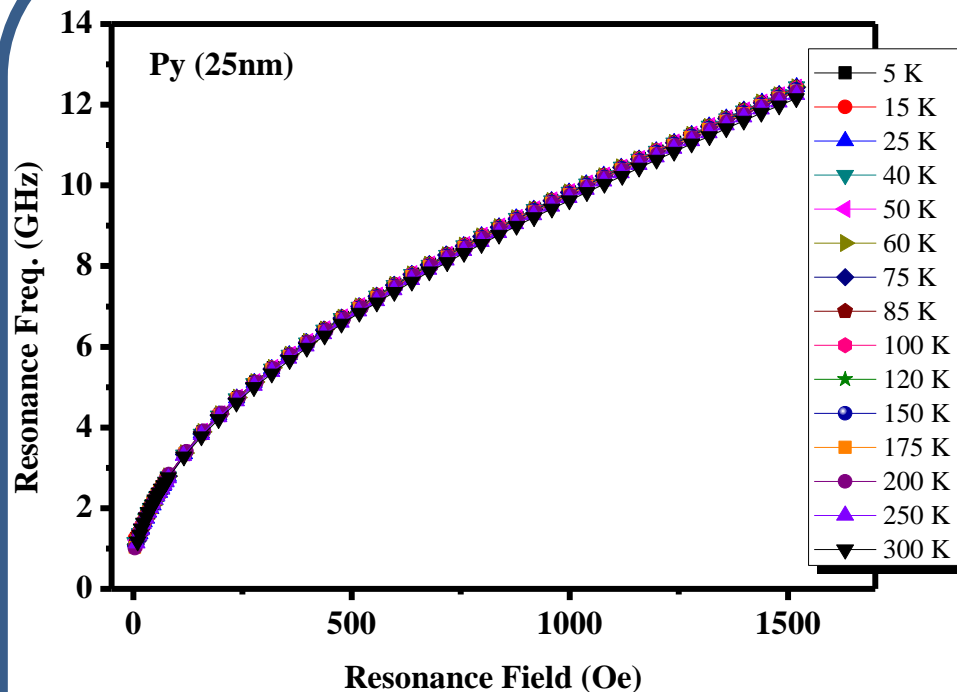


Magnetic field dependence of normalized resistivity for 20 nm (black) and 30 nm (red) samples at  $T = 5 \text{ K}$ . The black curve is shifted for clarity.

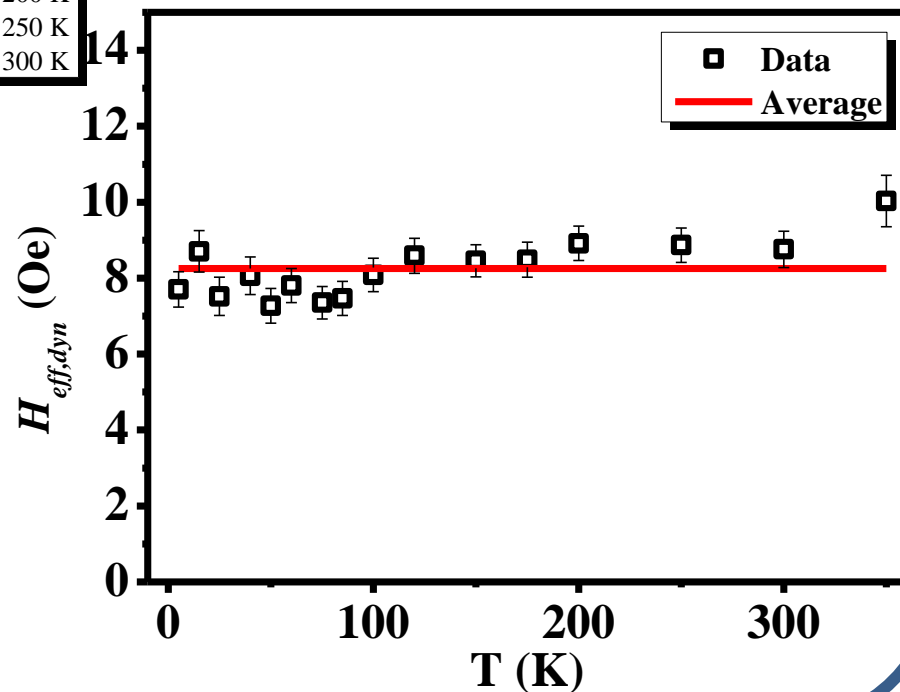
Temperature dependence of normalized resistivity for 30 nm sample measured under zero magnetic field. Inset shows the schematic illustration of the Fermi level.



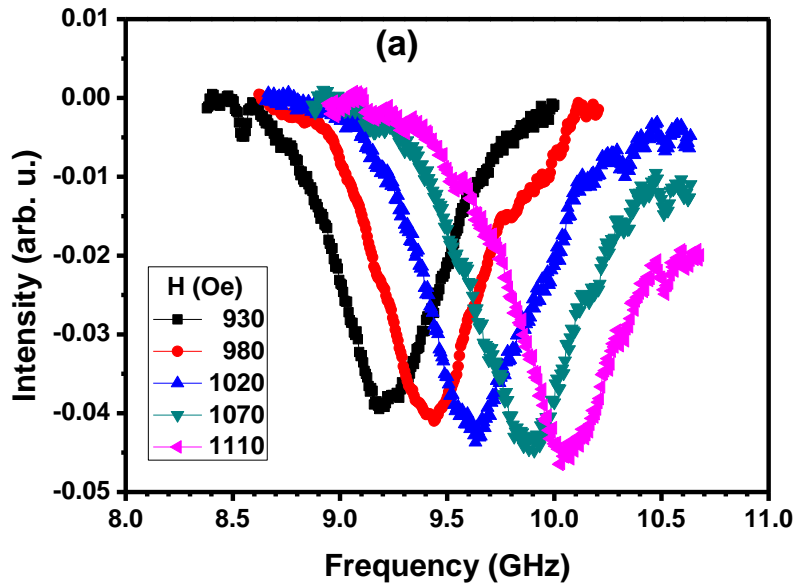
# FMR for Py (25nm) single layer



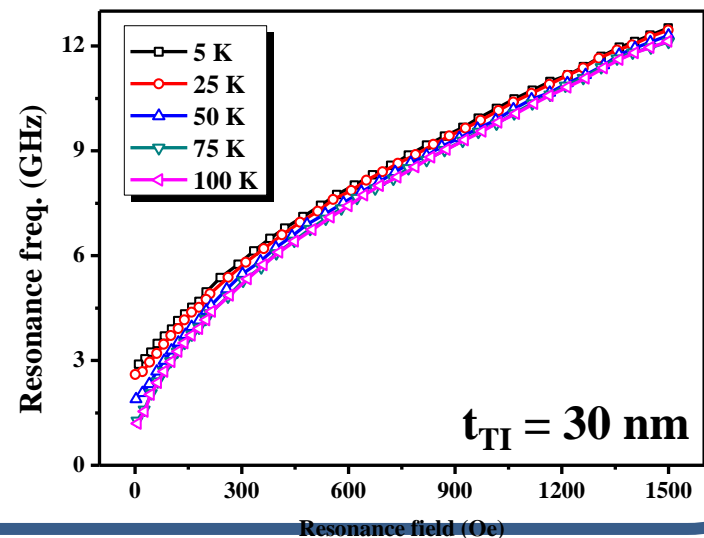
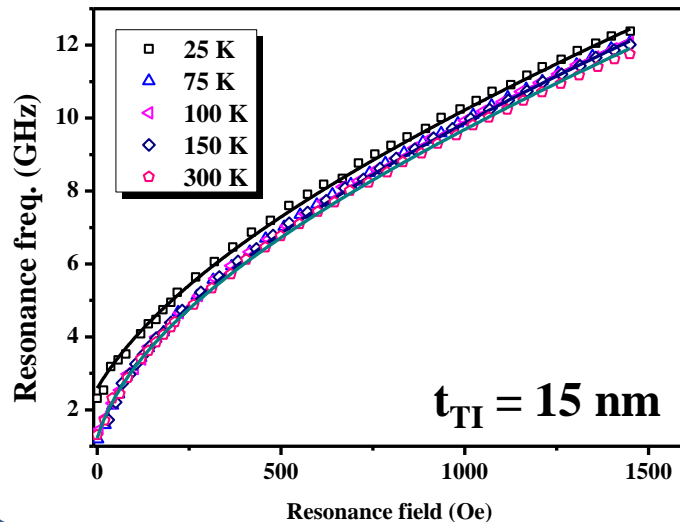
$$f_{res} = \frac{\gamma}{2\pi} \sqrt{H_{FMR} (H_{FMR} + 4\pi M_S)}$$

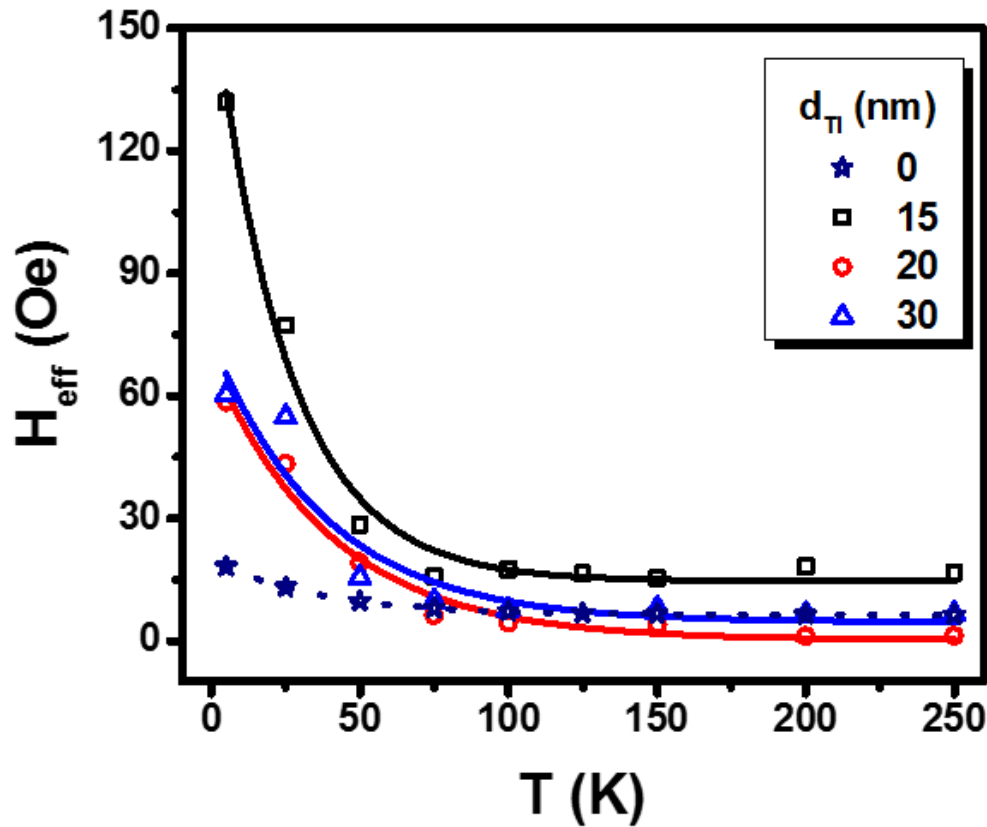


# FMR for $\text{Bi}_2\text{Te}_3/\text{Py}$ Bilayers



Temperature dependence measurements of FMR show upper left shift compared to single Py layers.





**Possible effects:**

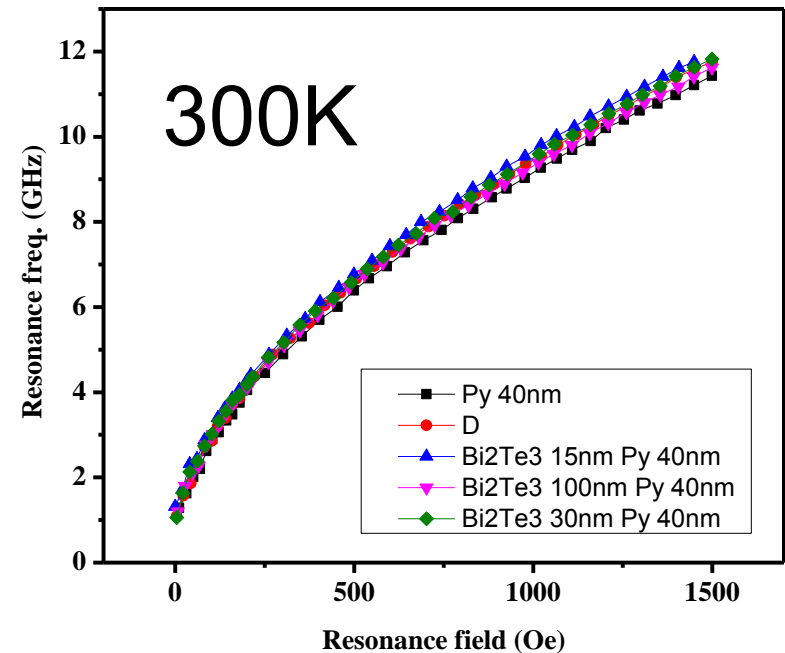
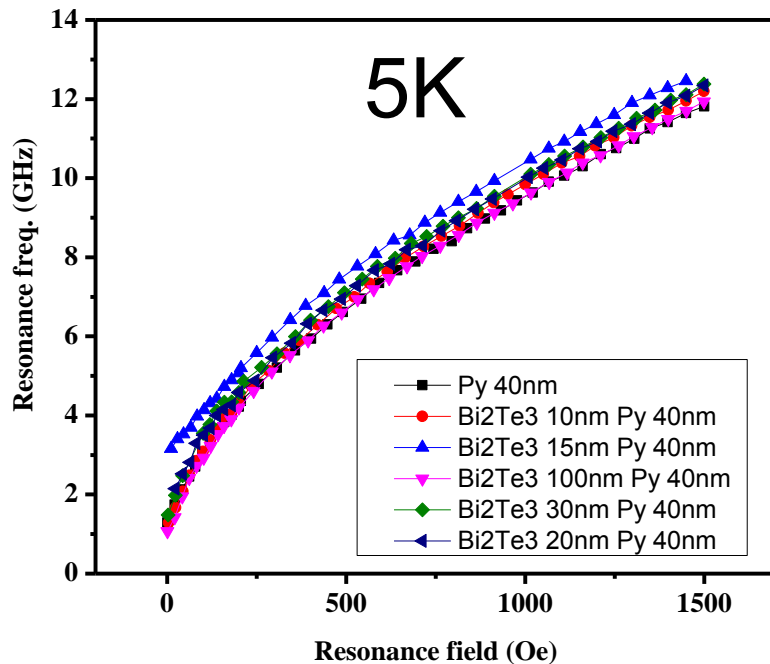
- FM-anisotropy
- proximity effect
- FM/TI exchange coupling.

$$f_{\text{res}} = \frac{\gamma}{2\pi} \sqrt{(H_0 + H_{\text{eff}})((H_0 + H_{\text{eff}}) + 4\pi M_S)}$$

Temperature dependence of the effective field for the reference sample and 15, 20, and 30 nm  $\text{Bi}_2\text{Te}_3$  samples. Solid lines are exponential fits.

# Bi<sub>2</sub>Te<sub>3</sub>/Py Bilayers

## Bi<sub>2</sub>Te<sub>3</sub> thickness dependence of FMR



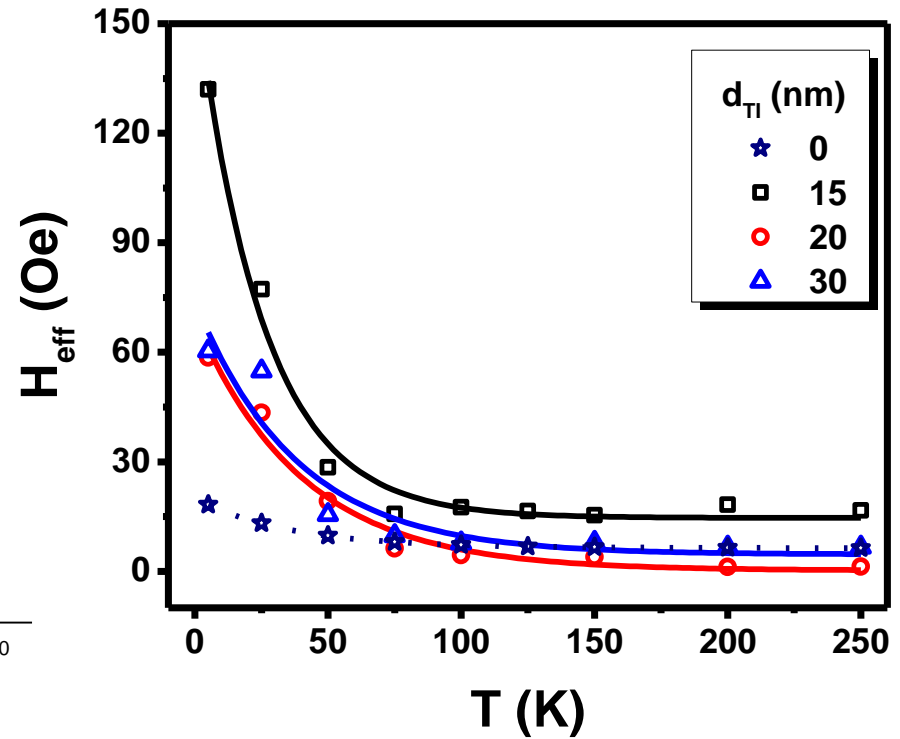
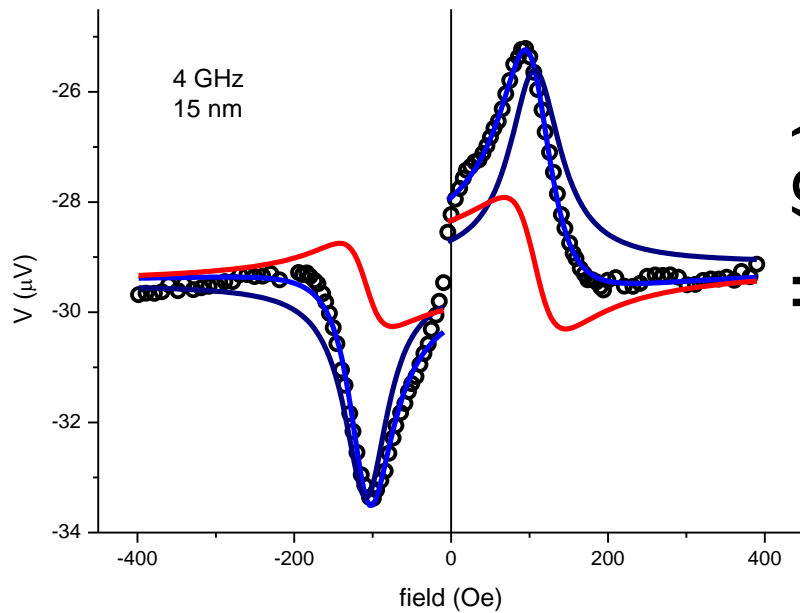
# Bi<sub>2</sub>Te<sub>3</sub>/Py Bilayers

H<sub>eff</sub> for Bi<sub>2</sub>Te<sub>3</sub> thickness dependence

	γ=1.8887E7 ; M <sub>s</sub> =8863.2 Oe (5K) γ=1.88264E7 ; M <sub>s</sub> =8271.3 Oe (300K)	
	5K	300K
Py (40nm)	18.26 $\pm$ 1 Oe	6.64 $\pm$ 1 Oe
Bi <sub>2</sub> Te <sub>3</sub> (10nm)/ Py (40nm)	27.79 $\pm$ 3.6 Oe	22.16 $\pm$ 3.43 Oe
Bi <sub>2</sub> Te <sub>3</sub> (15nm)/ Py (40nm)	132 $\pm$ 5.5Oe	44 $\pm$ 5.4Oe
Bi <sub>2</sub> Te <sub>3</sub> (20nm)/ Py (40nm)	58.5 $\pm$ 4.25Oe	-
Bi <sub>2</sub> Te <sub>3</sub> (30nm)/ Py (40nm)	60.344 $\pm$ 5.5Oe	29 $\pm$ 3.7Oe
Bi <sub>2</sub> Te <sub>3</sub> (100nm)/ Py (40nm)	12.17 $\pm$ 1.1 Oe	19.8 $\pm$ 1.9 Oe

# Summary

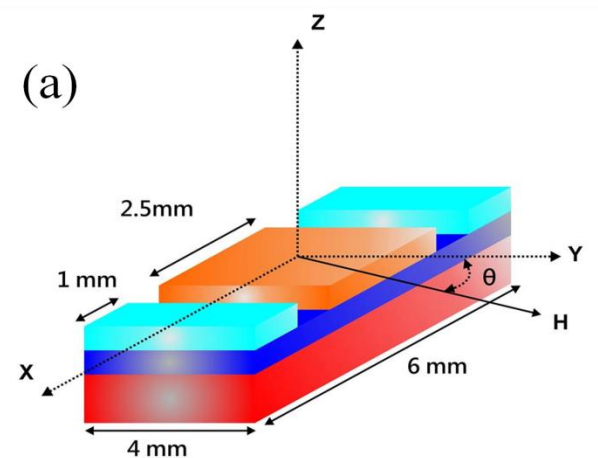
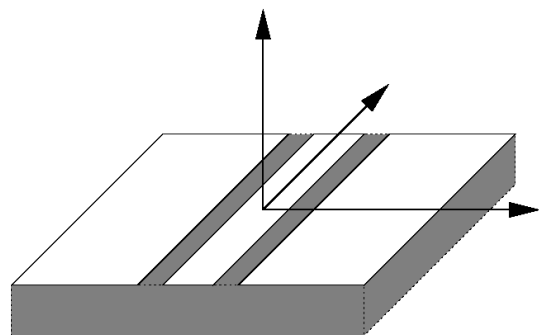
1. Large  $H_{\text{eff}}$  due to the spin pumping effect was observed for different  $\text{Bi}_2\text{Te}_3$  thin films.
2.  $H_{\text{eff}}$  has a maximum value around  $t_{\text{TI}} = 15\text{nm}$ .
3.  $H_{\text{eff}}$  decreases with temperature exponentially; characteristic temperature  $T_0 \sim 25\text{-}33\text{ K}$  is on the energy scale of  $2.5\text{ meV}$ .



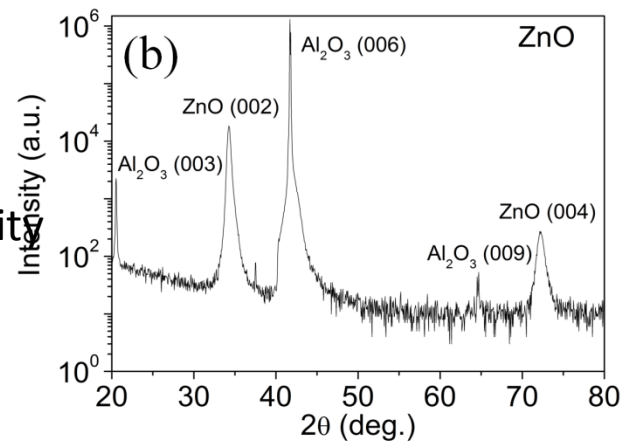
We observed an exchange coupling between NiFe and TI surface. The strength of this coupling decay with increasing temperature with a characteristic temperature  $\sim 25\text{K}$ , or  $\sim 2.2\text{ meV}$ .

# Our results on Spin Pumping in ZnO/Py film

co-planar waveguide

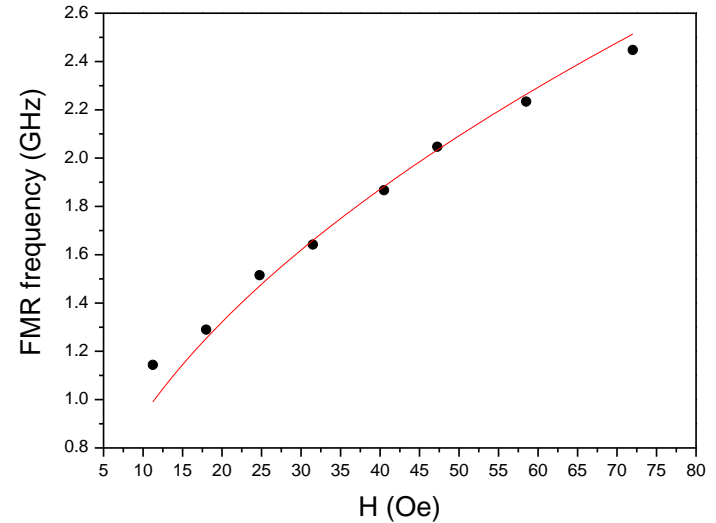
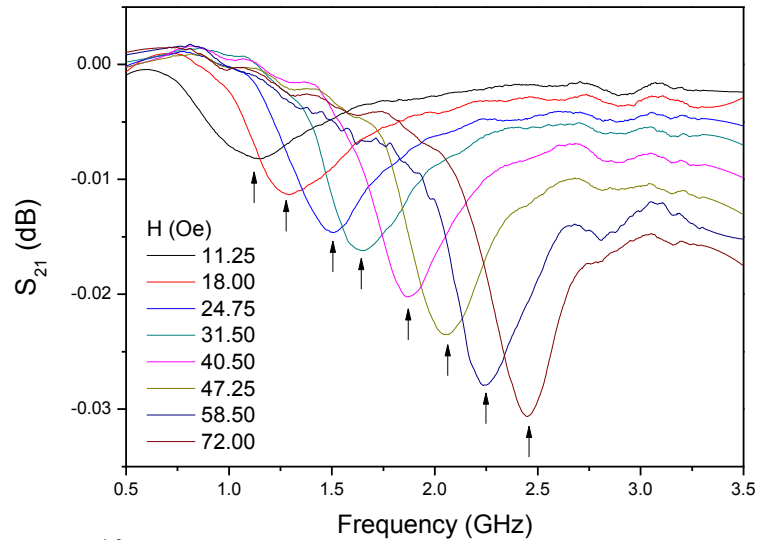


ZnO:  
Resistivity 0.014  $\Omega$ -cm  
carrier concentration  $6.09 \times 10^{18} \text{ cm}^{-3}$  mobility  
72.9  $\text{cm}^2/\text{V-s}$



“Inverse spin Hall effect induced by spin pumping into semiconducting ZnO” APL  
**104**, 052401 (2014)

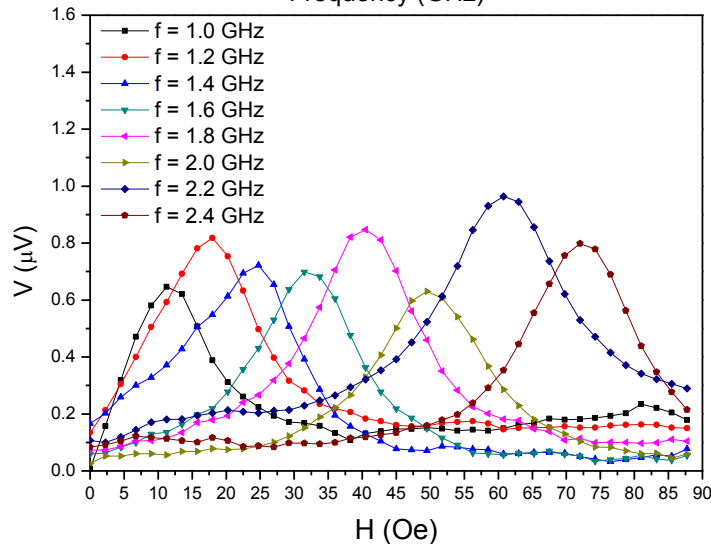
# The FMR spectra of ZnO/Py samples.



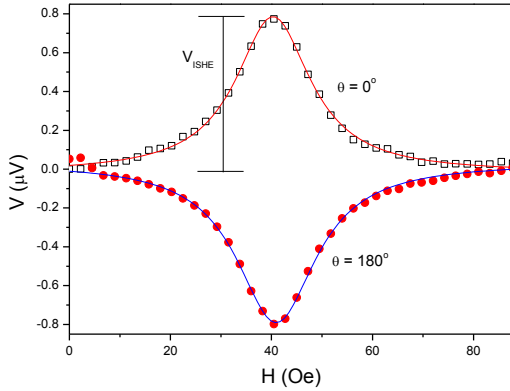
$$(f / \gamma)^2 = H_{\text{FMR}} (H_{\text{FMR}} + 4\pi M_s)$$

$$V = L \frac{\Delta H^2}{(H - H_0)^2 + \Delta H^2} + D \frac{\Delta H(H - H_0)}{(H - H_0)^2 + \Delta H^2},$$

Lorentz and dispersive line shapes



Magnetic field  $H$  dependence of electromotive force  $V$  measured for the  $\text{Ni}_{80}\text{Fe}_{20}/\text{ZnO}$  thin film under 50 mW microwave excitation.



$$\mathbf{E}_{ISHE} \propto \mathbf{J}_s \times \boldsymbol{\sigma}$$

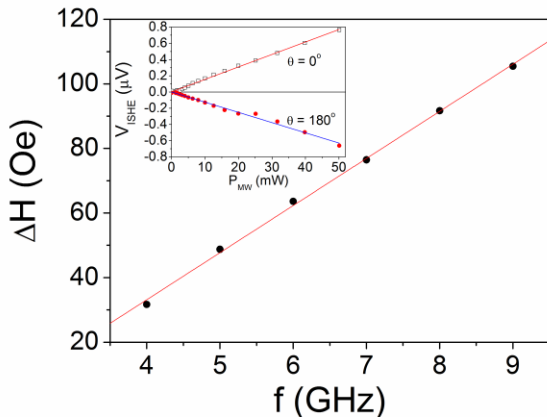
$$V_{ISHE} = \frac{W_F \theta_{SH} \lambda_N \tanh\left(\frac{d_N}{2\lambda_N}\right)}{d_N \sigma_N + d_F \sigma_F} \left(\frac{2e}{\hbar}\right) j_s^0$$

$$j_s^0 = \frac{g_r^{\uparrow\downarrow} \gamma^2 \hbar^2 \hbar [4\pi M_s \gamma + \sqrt{(4\pi M_s)^2 \gamma^2 + 4\omega^2}]}{8\pi \alpha^2 [(4\pi M_s)^2 \gamma^2 + 4\omega^2]}$$

Considering spin back flow,

$$E_y = \frac{2e/\hbar}{\sigma_N d_N + \sigma_F d_F} \left[ j_{1s}^z(0) \theta_{SH}^N \lambda_{sd}^N \tanh\left(\frac{d_N}{2\lambda_{sd}^N}\right) + j_{2s}^z(0) \theta_{SH}^F \lambda_{sd}^F \tanh\left(\frac{d_F}{2\lambda_{sd}^F}\right) \right]$$

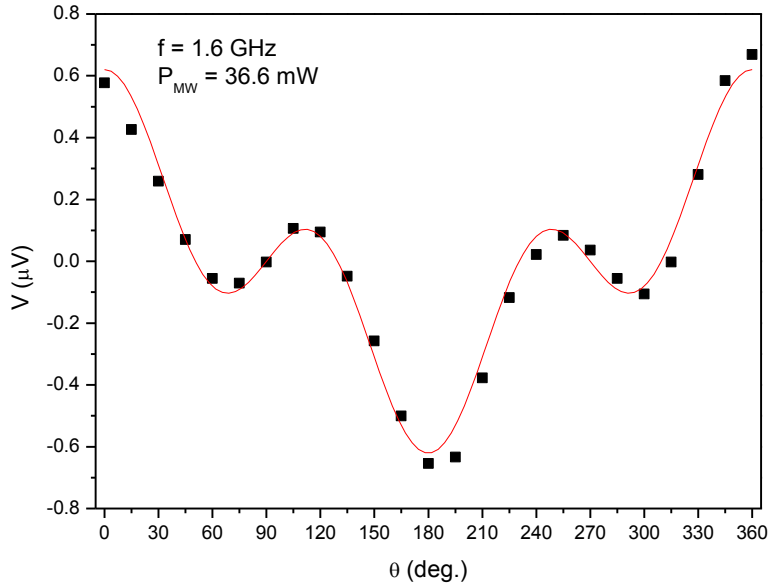
Spin mixing conductance  $g_s^{\uparrow\downarrow}$  is the essential parameter to the spin pumping experiment. It refers to the efficiency of generating a spin current



$$\alpha = \frac{g\mu_B}{4\pi M_s d_F} g_r^{\uparrow\downarrow}$$

$$\Delta H_{FMR} = \Delta H_0 + \frac{2\alpha}{\gamma} f$$

$$V_{dc}(H, \theta) = V_{AMR} [L(H) \cos \phi + L'(H) \sin \phi] \sin(2\theta) \sin \theta + V_{ISHE} L(H) \cos \theta$$



$$L(H) = \frac{\Delta H^2}{(H - H_{FMR})^2 + \Delta H^2}$$

$$L'(H) = \frac{\Delta H(H - H_{FMR})}{(H - H_{FMR})^2 + \Delta H^2}$$

The in-plane angle  $\theta$  dependence of the electromotive force  $V$  or  $\text{Ni}_{80}\text{Fe}_{20}/\text{ZnO}$  thin film. The solid symbols are the experimental data and the red line is the theoretical fitting line.

Magnonic charge pumping?  
[PRB 92, 024402 \(2015\)](https://doi.org/10.1103/PhysRevB.92.024402)

PHYSICAL REVIEW B 83, 144402 (2011)

**Spin pumping and anisotropic magnetoresistance voltages in magnetic bilayers:  
Theory and experiment**

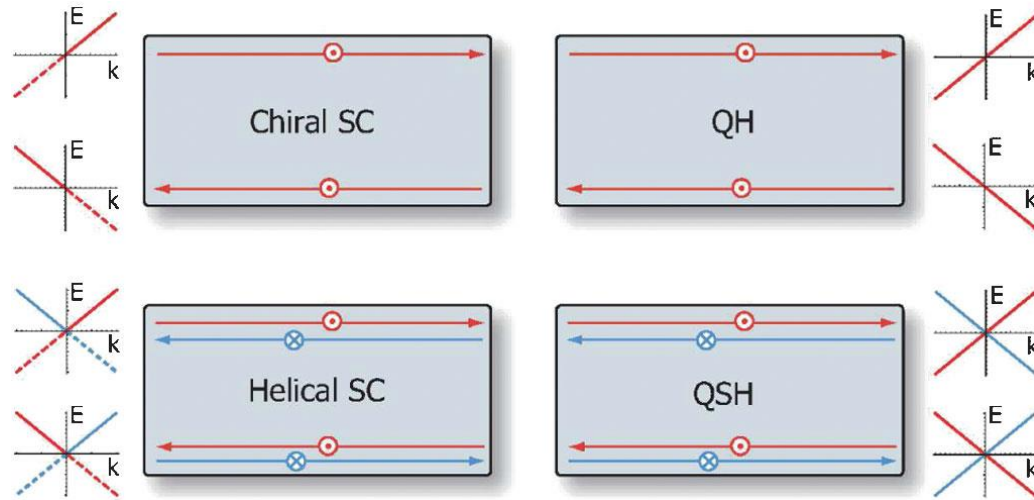
A. Azevedo,<sup>1,\*</sup> L. H. Vilela-Leão,<sup>1</sup> R. L. Rodríguez-Suárez,<sup>2</sup> A. F. Lacerda Santos,<sup>1</sup> and S. M. Rezende<sup>1</sup>

<sup>1</sup>Departamento de Física, Universidade Federal de Pernambuco, Recife, Pernambuco 50670-901, Brazil

<sup>2</sup>Facultad de Física, Pontificia Universidad Católica de Chile, Casilla 306, Santiago, Chile

(Received 6 June 2010; revised manuscript received 29 January 2011; published 4 April 2011)

# Topological insulators and topological superconductors

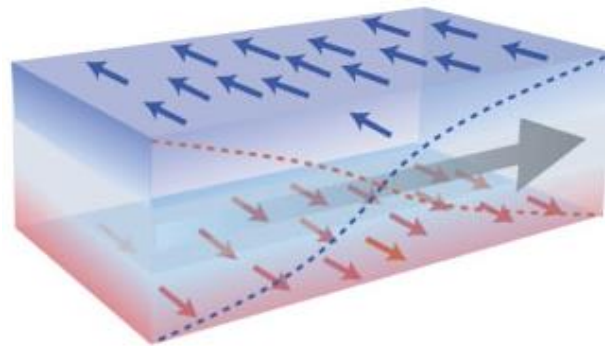
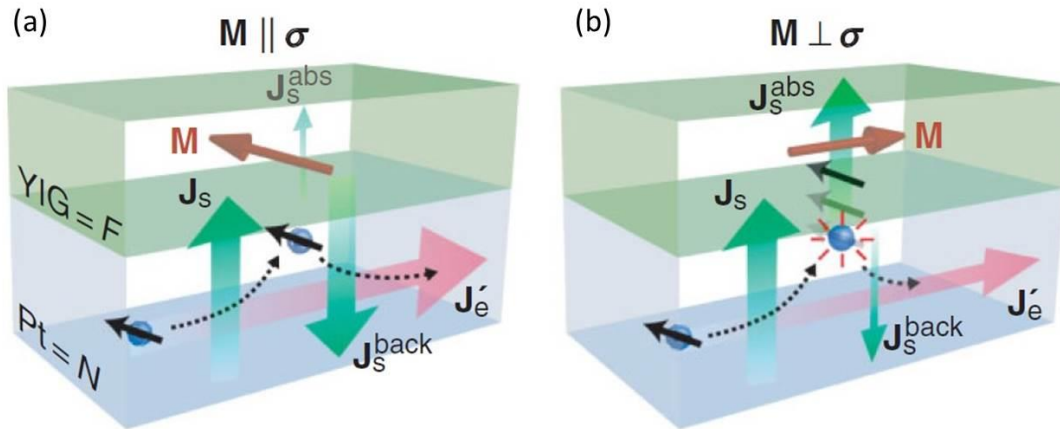


Schematic comparison of 2D chiral superconductor and QH states. In both systems, TR symmetry is broken and the edge states carry a definite chirality. (Bottom row) Schematic comparison of 2D TR invariant topological superconductor and QSH insulator. Both systems preserve TR symmetry and have a helical pair of edge states, where opposite spin states counterpropagate. The dashed lines show that the edge states of the superconductors are Majorana fermions so that the  $E < 0$  part of the quasiparticle spectrum is redundant. In terms of the edge state degrees of freedom, we have symbolically  $\text{QSH} = (\text{QH})^2 = (\text{helical SC})^2 = (\text{chiral SC})^4$ .  
 From Qi, Hughes et al., 2009a.

# Summary

- Giant Magnetoresistance, Tunneling Magnetoresistance
- Spin Transfer Torque
- Pure Spin current (no net charge current)
  - Spin Hall, Inverse Spin Hall effects
  - Spin Pumping effect
  - Spin Seebeck effect
- Micro and nano Magnetics
- Spin pumping into Topological Insulator, Topological Superconductor
- Spin logic
- Skyrmion
- Is Spintronics the next generation technology beyond 2020?  
There is no better candidate in sight?

# Spin Hall Magnetoresistance



PRL **110**, 206601 (2013) Spin Hall magnetoresistance induced by a Nonequilibrium Proximity Effect

Spintronics has evolved in many aspects other than material developments, including effects like Giant Magnetoresistance, Tunneling Magnetoresistance, Spin Transfer Torque, Spin Hall, Spin Pumping, Inverse Spin Hall, and more. The underlying idea was to investigate and manipulate the electron spin degree of freedom in addition to its charge in transport phenomena. However, charge transport is usually accompanied by Joule heating problem as the sizes of the electronics continue to shrink. Thus, devices that manipulate pure spin currents can be highly beneficial compared to traditional charge-based electronics. We now have “spin caloritronics”, where one exploits the interaction between heat transport and the charge/spin carriers.

Spin caloritronic effect, such as spin Seebeck effect, has attracted a great deal of attention recently. The difference in the chemical potentials of the spin-up and the spin-down electrons can cause a pure spin current. This pure spin current can be detected by Pt strips via the inverse spin-Hall effect. In most cases such studies have been made on ferromagnetic thin films on substrates. The mechanism of spin Seebeck effect has evolved from the above-mentioned intrinsic difference in the spin chemical potentials when it was first reported experimentally to magnon-phonon interaction through the substrate in recent publication. We use patterned ferromagnetic thin film to demonstrate the profound effect of a substrate on the spin-dependent thermal transport [1]. With different sample patterns and on varying the direction of temperature gradient, both longitudinal and transverse thermal voltages exhibit asymmetric instead of symmetric spin dependence. This unexpected behavior is due to an out-of-plane temperature gradient imposed by the thermal conduction through the substrate and the mixture of the anomalous Nernst effects. Only with substrate-free samples have we determined the intrinsic spin-dependent thermal transport with characteristics and field sensitivity similar to those of anisotropic magnetoresistance effect.